The gut environment regulates bacterial gene expression which modulates susceptibility to bacteriophage infection

Marta Lourenço, Lorenzo Chaffringeon, Quentin Lamy-Besnier, Marie Titécat, Thierry Pédron, Odile Sismeiro, Rachel Legendre, Hugo Varet, Jean-Yves J.-Y. Coppée, Marion Bérard, et al.

The gut environment regulates bacterial gene expression which modulates susceptibility to bacteriophage infection

Authors

Marta Lourenço[1,2#], Lorenzo Chaffringeon[1,3,4], Quentin Lamy-Besnier[1], Marie Titécat[1,5], Thierry Pédron[1], Odile Sismeiro[6], Rachel Legendre[6,7], Hugo Varet[6,7], Jean-Yves Coppée[6], Marion Bérard[8], Luisa De Sordi[1,3,4] and Laurent Debarbieux[1*]

Affiliations

1 Institut Pasteur, Université de Paris, CNRS UMR6047, Bacteriophage Bacterium Host, Paris F-75015 France

2 Sorbonne Université, Collège Doctoral, F-75005 Paris, France

3 Sorbonne Université, INSERM, Centre de Recherche St Antoine, UMRS_938, Paris, France

4 Paris Center for Microbiome Medicine (PaCeMM) FHU, AP-HP, Paris, Ile-de-France, France

5 Université de Lille, INSERM, CHU Lille, U1286-INFINITE-Institute for Translational Research in Inflammation, F-59000 Lille, France

6 Transcriptome and EpiGenome Platform, Biomics, Center for Technological Resources and Research (C2RT), Institut Pasteur, Université de Paris, Paris F-75015 France

7 Bioinformatics and Biostatistics Hub, Department of Computational Biology, Institut Pasteur, Université de Paris, Paris F-75015 France

8 Institut Pasteur, Université de Paris, DT, Animalerie Centrale, Centre de Gnotobiologie, 75724 Paris, France

present address: Department of Global Health, Institut Pasteur, Université de Paris, Paris F-75015 France

*** Lead author and correspondence**

laurent.debarbieux@pasteur.fr

Summary

Abundance and diversity of bacteria and their viral predators, bacteriophages (phages), in the digestive tract are associated with human health. Particularly intriguing is the long-term coexistence of these two antagonistic populations. We performed genome-wide RNA sequencing on a human enteroaggregative *Escherichia coli* isolate, to identify genes differentially expressed between *in vitro* conditions and in murine intestines. We experimentally demonstrated that four of these differentially expressed genes modified the interactions between *E. coli* and three virulent phages by either increasing or decreasing its susceptibility/resistance pattern and also by interfering with biofilm formation. Therefore, the regulation of bacterial genes expression during the colonization of the digestive tract influences the coexistence of phages and bacteria, highlighting the intricacy of tripartite relationships between phages, bacteria and the animal host in intestinal homeostasis.

Introduction

The microbiota of the mammalian gut includes bacteria and their viral predators, bacteriophages (phages). In healthy individuals, these two antagonistic populations generally remain stable over time, but variations in their density and diversity have been associated with several human diseases or disorders (Gregory et al., 2020; Manrique et al., 2017; Mirzaei and Maurice, 2017; Shkoporov et al., 2019; Zuo et al., 2020). The long-term coexistence of populations of phages and bacteria *in vivo* probably results from a combination of mechanisms deployed by each of the three partners: phages, bacteria and the host (Kirsch et al., 2021; Mirzaei and Maurice, 2017).

Multiple molecular mechanisms regulate the dynamics of phage-bacterium interactions. These include mutations of genes encoding phage receptors to prevent attachment, restriction-modification enzymes and CRISPR systems, to degrade phage genomes, mutations of genes encoding proteins essential for phage infection and replication, abortive infection and superinfection exclusion systems (Labrie et al., 2010). Genome data mining has recently identified a growing number of

bacterial genes involved in phage defence systems experimentally tested only *in vitro* (Bernheim and Sorek, 2020; Millman et al., 2020; Rousset et al., 2021). In addition, other mechanisms, such as phenotypic resistance, a reversible state providing bacteria with temporary resistance to phages (Bull et al., 2014; Chapman-McQuiston and Wu, 2008; Levin et al., 2013), and leaky resistance (Chaudhry et al., 2018), have been proposed as means of prolonging the coexistence of phages and bacteria in microcosms *in vitro*. Moreover, abiotic (temperature, oxygen, nutrients) and biotic (microbial and mammalian cells) factors have been shown to influence phage-bacterium interactions in both *in vitro* and *in vivo* environments (Alseth et al., 2019; Golec et al., 2014; Hadas et al., 1997; Labedan, 1984; Lourenço et al., 2020; Scanlan et al., 2019; Sillankorva et al., 2004). However, the relevance and preponderance of these mechanisms in the mammalian gut remain poorly explored (Cornuault et al., 2020; De Sordi et al., 2019).

Bacteria modulate gene expression during their establishment in the digestive tract of mammals. Whether and how this could affect their susceptibility to phages remains unknown. However, there have been several observations indicating that phages with a similar efficacy *in vitro* behave differently in the gastrointestinal tract of mice (Maura and Debarbieux, 2012; Weiss et al., 2009). Likewise, we showed that phage replication in homogenized intestinal sections from colonized mice (*ex vivo*) is different not only from that *in vitro* but also between different gut sections (Galtier et al., 2017; Lourenço *et al.*, 2020; Maura et al., 2012a). These findings suggest that the gut environment modulates phage-bacterium interactions.

Here, we aimed to identify bacterial genes for which regulation within the digestive tract modifies bacterial susceptibility to phages. We performed a genome-wide transcriptomic analysis comparing *in vitro* and *in vivo* conditions for the *Escherichia coli* strain 55989. This strain is an enteroaggregative O104:H4 clinical isolate (EAEC pathotype frequently associated with traveller's diarrhoea) (Lääveri et al., 2020) that is known to form biofilms and that carries a pAA plasmid encoding virulence

79 determinants (Touchon et al., 2009). We previously isolated and characterized three virulent phages
80 (*Podoviridae* CLB_P1, *Myoviridae* CLB_P2 and *Siphoviridae* CLB_P3) infecting strain 55989 (Maura et
81 al., 2012b). Associated in a cocktail, these three phages rapidly decreased the intestinal load of strain
82 55989 colonizing the gut of conventional mice (Maura *et al.*, 2012a), before to promote a long-term
83 coexistence with this strain (Maura *et al.*, 2012b).
84
85 We identified chromosome- and plasmid-encoded genes differentially expressed by the *E. coli* strain
86 55989 during gut colonisation, encoding proteins with functions relating to iron acquisition, aerobic
87 and anaerobic respiration, sugar metabolism, motility, adhesion, aggregation, biofilm regulation and
88 LPS biosynthesis. We studied four of these genes (*bssR*, *fliA*, *lsrC* and *rfaL*), encoding proteins with
89 functions expected to affect phage-bacterium interactions. Using a combination of phenotypic assays
90 we experimentally confirmed that each of these four genes modulated phage-bacterium interactions
91 for at least one of the phages. This study reveals a molecular mechanism, ie the modification of
92 bacterial gene expression by the gut environment, which influences the susceptibility of bacteria to
93 phages, thereby contributing to the coexistence of these two antagonistic populations.
94

95 ## Results

96 **The efficacy of phage replication on *E. coli* cells grown *in vitro* differs from homogenized *E. coli*-**
97 **colonized gut samples**
98 We previously tested individually the ability of phages CLB_P1, CLB_P2 and CLB_P3 to establish a
99 long-term coexistence with the strain 55989 colonizing conventional mice. Each of these phages
100 behave differently. Phage CLB_P2 lasted over four weeks, while CLP_P3 and CLB_P1 fell below the
101 threshold of detection after eleven and four days, respectively (Maura and Debarbieux, 2012). These
102 data together with *in vitro* and *ex vivo* phage replication assays performed on 55989 cells (Maura *et*
103 *al.*, 2012a) supported the hypothesis that the regulation of bacterial genes may influence phage-
104 bacteria interactions. To test this hypothesis, we aimed to perform *in vivo* transcriptomics on

105 samples from monocolonized mice (axenic mice colonized only with strain 55989). First, we assessed
106 the individual phage replication on 55989 cells recovered from homogenized gut sections (ileum and
107 colon) of monocolonized mice, as well as on 55989 cells collected from liquid medium during the
108 exponential and stationary growth phases (Fig. 1). As a control, we tested the stability of the three
109 phages in absence of strain 55989 and found that during the assay (5 h) the number of phages
110 decreased by about 1-log in LB and gut samples from axenic mice (Fig. 1, left). We also evaluated the
111 behaviour of exponential and stationary grown 55989 cells when added to gut homogenates from
112 axenic mice during 5 h. We found that exponentially grown cells were capable to grow by about 2-log
113 in both ileum and colon sections, while stationary grown cells could not (Fig 1, right).
114 The three phages displayed an amplification of three to four orders of magnitude relative to the
115 initial phage dose on exponentially growing 55989 cells (Fig. 1, central). In sharp contrast, the level of
116 phages CLB_P1 and CLB_P3 recovered after incubation with cells collected during the stationary
117 growth phase was several orders of magnitude lower than the initial dose, showing that these
118 phages did not amplify, whereas phage CLB_P2 displayed a moderately impaired amplification (two
119 orders of magnitude lower compared to the exponential growth condition) (Fig. 1 central part). The
120 strong reduction of the amount of recovered phage CLB_P1 upon incubation with stationary cells
121 suggests that it binds to cells but is unable to infect them. A similar situation was previously reported
122 for phage T7 exposed to *E. coli* cells lacking *flhDC* and overexpressing curli in biofilms (Vidakovic et
123 al., 2018). Perhaps, the inability of phage CLB_P1 to persist in the murine gut could be linked to its
124 inability to infect 55989 cells colonizing the gut of mice.
125 On homogenized ileal samples from monocolonized mice, the three phages amplified to a similar
126 degree to cells collected during exponential growth. On colon samples from monocolonized mice,
127 CLB_P2 and CLB_P3 amplification were similar to that on ileal samples, but the amplification of
128 CLB_P1 was strongly reduced by 4-log (Fig. 1 central part). These data are consistent with a previous
129 assessment of the amplification of these phages in intestinal sections collected from conventional
130 mice colonized with strain 55989, demonstrating that the presence of other microbes was not

involved in the differences observed between *in vitro* and *ex vivo* conditions (Maura *et al.*, 2012a). Therefore, the replication of each of the three phages was differentially affected by the growth of strain 55989 in different environments. Since the regulation of gene expression is a hallmark of the adaptation of bacteria to changing environments, we next looked for relationships between bacterial gene expression and phage-bacterium interactions.

E. coli strain 55989 experiences metabolic shifts during gut colonisation

For identification of the set of genes from strain 55989 specifically expressed in the gut, we compared the genome-wide pool of mRNAs extracted in three sets of growth conditions: i) *in vitro* exponential growth (OD_{600}=0.5; "exponential" samples *n*=4); ii) *in vitro* stationary growth (equivalent OD_{600}=5; "stationary" samples *n*=4); iii) *in vivo* growth in the colon of monocolonized mice ("colon" samples *n*=4; see methods). A principal component analysis (PCA) showed that the three conditions were very different and, within each condition, the replicates were very similar resulting in a remarkable differentiation and supporting further analysis (Fig. 2A). Interestingly, the global gene expression pattern of colon samples was more similar to exponential samples than to stationary samples (Fig. 2B). We then compared the transcriptomes of the colon with exponential and stationary samples separately, to identify the set of genes differentially expressed between these sets of conditions (Fig. 2C). Next, we cross-checked genes from these comparisons with the differential expressed genes between exponential and stationary samples to remove those in common and identify genes differentially expressed during the growth of strain 55989 in the colon. We obtained a list of 156 over and 53 underexpressed genes, the functions of which were determined using a Gene Ontology analysis (http://geneontology.org/) and the EcoCyc database (Keseler et al., 2011) (Tables S1 and S2).

A large proportion of the functions of genes overexpressed in the colon concerned sugar metabolism and transport (Fig. 3A and Table S1A). The most significantly overexpressed gene, *ompG*, encodes a

specific porin involved in carbohydrate transport (Fajardo et al., 1998). Several carbohydrate pathways (sucrose, gluconate, glucurate, galactarate and galactonate) were overexpressed, consistent with previous reports of *E. coli* adaptation to the gut environment (Conway and Cohen, 2015; Fabich et al., 2008; Lourenço et al., 2016). We also found that genes involved in carnitine metabolism (*fixA*, *fixB*, *fixC* and *caiT*), were overexpressed. Furthermore, genes involved in the utilization of ethanolamine (*eutN*, *eutG*, *eutJ* and *eutP*) were overexpressed.

As expected, we observed differential expression for genes involved in the transition from aerobic to anaerobic environments. Together with the genes involved in carnitine metabolism, the *frdBCD* genes encoding the fumarate reductase, and *fumB,* encoding a fumarase were all found to be overexpressed, as previously reported (Condon and Weiner, 1988; Meadows and Wargo, 2015; Woods and Guest, 1987). Conversely, the full operon *cyoABCDE*, encoding the subunits of the cytochrome bo terminal oxidase and haem O synthase, was strongly underexpressed, a hallmark of decreased oxygen availability (Fig. 3B and Table S1B) (Cotter et al., 1990). The second most significantly underexpressed set of genes was related to iron acquisition and included enterobactin biosynthesis and export genes (*entC*, *entS*, *fepD*, *fhuD*), together with *fecI*, *yncD* and *yncE* genes, all of which encode proteins with functions relating to iron transport. These observations validated our approach to identify bacterial genes whose expression could affect phage-bacteria interactions in the gut, but also highlighted a number of specific features putatively involved in the intestinal colonization process of this enteroaggregative *E. coli* strain and that require further investigations.

Plasmid-encoded virulence determinants are upregulated during *E. coli* growth in the gut

The EAEC strain 55989 carries a plasmid (p55989) from the pAA family (Croxen and Finlay, 2010) that harbours several genes encoding factors involved in adhesion to epithelial cells (Boll et al., 2017; Weintraub, 2007). In our analysis of *in vivo* differentially expressed plasmid-encoded genes, we identified seven overexpressed genes, four of them with functions relating to adhesion (*agg3B*, *agg3C, agg3D* and *p55989_0069*) (Fig. S1; Table S1C), consistent with the phenotype of EAEC strains,

183 which form aggregates at the surface of intestinal cells. We also found two plasmid genes encoding
184 putative transposases to be overexpressed, consistent with the mechanisms involved in the genetic
185 adaptation of *E. coli* cells to the gut environment (Barroso-Batista et al., 2014; Lourenço *et al.*, 2016).
186 Regarding other mobile genetic elements, the *in silico* analysis of the genome of strain 55989
187 revealed that it contains seven intact prophage regions, one incomplete and one questionable (see
188 methods). None of these regions were differentially expressed in our RNA-Seq data.
189
190 **Comparative transcriptomic analysis highlights bacterial genes related to phage infection**
191 Since phage replication is altered in both stationary phase and colon compared to exponential phase
192 samples (Fig. 1), we analysed the above transcriptomics dataset by performing pairwise comparisons
193 between exponential phase with either colon or stationary phase samples in order to identify genes
194 potentially linked to these changes in phage replication. Then, we removed genes differentially
195 expressed between colon and stationary phase samples (see methods and Fig. 2D). In total, 238
196 genes (73 overexpressed and 143 underexpressed) were identified, about 50% of which have no
197 known function (Table S1D and S1E, respectively). The underexpressed genes (Table S1E) with known
198 functions included genes involved in the biosynthetic pathway for flagella (including *fliA*) and LPS
199 (including *rfaL*), both of which act as cell wall receptors for phages (Choi et al., 2013; Feugeas et al.,
200 2016; Shin et al., 2012). All genes encoding proteins involved in the flagellum apparatus were indeed
201 underexpressed, suggesting that phages relying on this structure for entry would less efficiently
202 infect strain 55989 in both stationary phase and colonic samples. None of the overexpressed genes
203 with known functions were previously associated with phage infection (Table S1D). However, the
204 most significantly overexpressed gene, *bssR*, has been implicated in biofilm formation, and another
205 two genes (*lsrC* and *ego*) are involved in the import of autoinducer-2, a quorum sensing molecule.
206 Interestingly, the function of these genes is related to bacterial community lifestyle and could
207 possibly affect phage-bacterium interactions as previously shown for *Vibrio cholera* (Hoque et al.,

2016; Pires et al., 2021). Therefore, we experimentally tested the contribution of these four gene (*bssR*, *fliA*, *lsrC* and *rfaL*) to the infectivity of each of the three phages.

The impact on phage-bacterium interactions of the two underexpressed genes, *fliA*, the master regulator of flagellum assembly (Helmann and Chamberlin, 1987) and *rfaL* (also known as *waaL*), encoding the O-antigen ligase (Klena et al., 1992), was assessed using 55989 strains in which either gene was deleted (55989Δ*fliA* and 55989Δ*rfaL*). To investigate the role of the two overexpressed genes, *bssR*, which encodes a global transcriptional regulator involved in biofilm formation (Domka et al., 2006), and *lsrC*, which encodes a subunit of the autoinducer-2 membrane transporter (Xavier and Bassler, 2005), we introduced a plasmid carrying either of these genes, under the control of an IPTG-inducible promoter, into strain 55989.

The lack of *rfaL* decreases the susceptibility of strain 55989 to phage CLB_P1

We first assessed the efficiency of plating (EOP) of phage CLB_P1 and found that it dropped by 3-log (2.10×10^{-3} +/- 3.11×10^{-4}) on the 55989Δ*rfaL* strain, but remained unchanged in the 55989Δ*fliA* strain (1.19 +/- 0.28) as well as in the strain 55989 overexpressing either *bssR* (1.08 +/- 0.33) or *lsrC* (1.18 +/- 0.45) genes. The growth and lysis of cells over time in liquid medium following exposure to phage CLB_P1 confirmed these results with notably the lack of lysis of the 55989Δ*rfaL* strain (Fig. 4A,B). As *rfaL* encodes the O-antigen ligase we hypothesized that the O-antigen could act as a receptor for this phage. In fact, phage CLB_P1 could not bind to the 55989Δ*rfaL* strain compared to either the WT or the 55989Δ*fliA* strain (Fig 4C,D,E). Moreover, cells aggregation by a O104 serotype specific antibody was prevented when 55989 cells were incubated with phage CLB_P1 but not with another unrelated phage, showing that phage CLB_P1 recognizes the O-antigen part of the LPS as a receptor (Fig 4F). We then evaluated the impact of phage CLB_P1 when added to 24 h-old biofilms formed by either 55989Δ*fliA*, 55989Δ*rfaL*, 55989-p*bssR* or 55989-p*lsrC* strains (Fig. S2). The overexpression of either *bssR* or *lsrC* genes had no significant effect on the amount of biofilm produced compared to the strain 55989 carrying the empty plasmid between 24 and 48 h in absence

234 or presence of phage CLB_P1 as assessed by crystal violet quantification (Fig. S2A and Table S2A and
235 S2B). Likewise, the amount of CFUs recovered at 48 h from the corresponding experiments did not
236 revealed any significant differences (Fig. S2B and Table S2A and S2B). We obtained similar results
237 with 55989Δ*fliA* and 55989Δ*rfaL* strains (Fig. S2C,D and Table S2A and S2B). In conclusion, these data
238 show that the downregulation of *rfaL* when 55989 cells inhabit the colon of mice likely impairs their
239 infection by phage CLB_P1, which by itself does not affect biofilm formation.
240
241 **Phage CLB_P2 infection is insensitive to the lack of *rfaL* or *fliA* genes as well as the overexpression**
242 **of *bssR* or *lsrC* genes**
243 Neither the EOP of CLB_P2 (Table S2C) nor the lysis of 55989Δ*fliA* or 55989Δ*rfaL* strains, or the lysis
244 of 55989 cells carrying the plasmids p*bssR* or p*lsrC*, was affected in comparison to their
245 corresponding control strains (WT and p*empty*), showing that none of these genes interfere with
246 CLB_P2 infection in these growth conditions (Fig. 5A,B). Unexpectedly, the presence of CLB_P2
247 significantly increased the amount of biofilm when either *bssR* (p=0.0029) or *lsrC* (p=0.0007) were
248 IPTG-induced, in comparison with the control strain (Fig 5C and Table S2A). This was not correlated
249 to changes of CFUs in the overexpressing strains compared to the control (Fig 5D and Table S2B). We
250 even noticed that the presence of CLB_P2 led to a significant reduction of the level of CFUs of all
251 strains compared to its absence (p=0.005 and below) (Fig. 5D and Table S2B). This moderate drop of
252 1 to 2-logs of CFUs indicates that some phage CLB_P2 infected cells embedded in the biofilm matrix.
253 We hypothesize that this phage displays some affinity to the biofilm matrix, which leads to carry over
254 some particles during the washing steps before cells are resuspended and mixed with this residual
255 phage population. This was further supported by the data obtained from biofilm assays performed
256 with 55989Δ*fliA* or 55989Δ*rfaL* strains and their plasmid-complemented counterparts. For all of
257 these strains phage CLB_P2 did not change the amount of biofilms produced but its presence led
258 again to a significant reduction of the level of CFUs recovered (Fig. S3AB and Table S2A and S2B).
259 Therefore, none of the four candidate genes were affecting the capacity of phage CLB_P2 to infect

55989 cells, but we uncovered that the presence of CLB_P2 increases biofilm formation by cells overexpressing genes related to community lifestyle, perhaps as a defence response against this phage.

Phage CLB_P3 strongly promotes biofilm formation of 55989Δ*fliA* and 55989Δ*rfaL* strains

The EOP of phage CLB_P3 (Table S2C) on strain 55989Δ*rfaL* was slightly higher compared to the control, while it remains unchanged for the strains 55989Δ*fliA,* 55989p*bssR* and 55989p*lsrC*. The lysis kinetics of strain 55989Δ*rfaL* by CLB_P3 was not affected during early time points in contrast to late time points, compared to all the other strains tested that were not different from their respective controls (WT and p*empty*) (Fig 6A,B). We then observed that the presence of CLB_P3 significantly increased the amount of biofilm formed by both the 55989Δ*fliA* (p=0.0040) and 55989Δ*rfaL* (p<0.0001) strains (Fig 6C and Table S2B). Particularly surprising was the amount of biofilm formed by the 55989Δ*rfaL* strain that increased by a factor of 5 on the OD scale compared to the highest values observed in all the other conditions tested (0.1 vs 0.02). When *trans*-complemented with a plasmid expressing either *fliA* or *rfaL*, the corresponding defective strains formed as much biofilm as the wild type strain (Fig. 6C). This large increase in biofilms was not correlated to an increase in CFUs (Fig 6D and Table S2C). Moreover, adsorption assays of phage CLB_P3 revealed that its affinity to each of the 55989Δ*fliA* and the 55989Δ*rfaL* strains was nearly 1-log lower compared to wild type strain, excluding the hypothesis that a stronger binding of this phage elicits an elevated biofilm formation (Fig. S4). In contrast, no significant impact of phage CLB_P3 was observed on the amount of biofilms formed by strains overexpressing either *bssR* or *lsrC* (Fig. S5A and Table S2A). Nevertheless, the amount of CFUs recovered from 55989 p*lsrC* biofilms exposed to CLB_P3 was significantly higher compared to the corresponding control cells (p=0.0016), a result that is the opposite of those obtained with phage CLB_P2 (Fig. S5B and Table S2B). Here we found that cells that are lacking either *fliA* or *rfaL* genes strongly increase biofilm formation only in presence of phage CLB_P3, perhaps eliciting a phage defence system.

The replication of phage CLB_P1 is abolished in the ileum of 55989Δ*rfaL*-colonized mice.

The two strongest phenotypes associated to the four gene candidates were observed with phage CLB_P1 that is severely impaired in infecting 55989Δ*rfaL* cells, and phage CLB_P3 that is strongly promoting biofilm formation of both 55989Δ*fliA* and 55989Δ*rfaL* cells. We then asked to which extent these phenotypes would translate into modifications of phage-bacteria interactions in the mouse gut. For this we tested the *ex vivo* replication of the three phages (CLB_P2 serving as a control phage) in intestinal organs from 55989Δ*fliA*- and 55989Δ*rfaL*-colonized mice. As expected, we found that the amplification of phage CLB_P1 is strongly affected on ileal and colonic homogenates from 55989Δ*rfaL*-colonized mice, compared to phages CLB_P2 and CLB_P3 (Fig. 7). These data demonstrate that a 3-log reduction of the EOP observed *in vitro* translates into a weak replication in organ homogenates, preventing the further *in vivo* evaluation of phage CLB_P1. Results obtained with homogenates from 55989Δ*fliA*-colonized mice were not dissimilar to those obtained from wild-type-colonized mice for the three phages (Fig. 1) showing that this gene has no impact on phage infection in organs (Fig. 7). Therefore, the increased biofilm formation promoted by the presence of CLB_P3 during the *in vitro* assays does not translate into an impaired phage infection in organs. Nevertheless, during this assay we observed that the number of CFUs of the 55989Δ*fliA* strain did not increase in the colon compared to the ileal samples. This suggests that some genes under *fliA* regulation may be required for optimal growth in this gut section. This could also explain the trend of a lower amplification in colon compared to ileal sections observed with the three phages.

Discussion

Bacteria and virulent phages coexist over time in the digestive tract of mammals, raising questions about the predator-prey dynamics of these two antagonistic populations (Lourenço *et al.*, 2020; Mirzaei and Maurice, 2017). Here, we investigated whether the regulation of bacterial gene expression occurring during their colonisation of the gut environment affects their susceptibility to

phages (Lourenço et al., 2018). We performed a genome-wide transcriptomic analysis of *E. coli* strain 55989, an enteroaggregative pathogenic strain for which we had already characterised three virulent phages, CLB_P1, CLB_P2 and CLB_P3.

Comparisons of the transcriptomics data from colon samples with exponentially and stationary grown cells revealed the differential expression of several genes. Besides expected genes related to anaerobic growth as well as sugar metabolism and transport in the gut, we identified some genes related to host adaptation. For instance, the overexpression of *ompG* implies the activation of the transcriptional regulator *ycjW* (Luhachack et al., 2019), which in turns also regulates the production of H_2S, which has been shown to protect pathogens against the host immune response (Toliver-Kinsky et al., 2019). We also report the overexpression of genes involved in the metabolism of carnitine and ethanolamine, which are compounds derived from the host cells membrane. Both are known to play roles in the gut microbiota with carnitine being used for osmoprotection or as a source of nutrients (Meadows and Wargo, 2015), while ethanolamine has been previously shown to be used by enteroaggregative *E. coli* for improving its ability to outcompete commensal *E. coli* (Bertin et al., 2011). Amongst underexpressed genes we found several iron acquision systems, including enterobactin. This counterintuitive observation, since it is well established that iron acquisition systems are required for gut colonisation (Deriu et al., 2013), must be counterbalanced by the diversity of multiple iron acquisition systems identified in *E. coli* genomes, some of which, like Feo, are expressed in anaerobic conditions (Lau et al., 2016). Moreover, *fumB*, the expression of which decreases in conditions of iron limitation, was found to be overexpressed in the colon, suggesting that iron supply was not limiting in our experimental conditions (Fig. 3A and Table S1A). In addition, the analysis of the 55989 plasmid-encoded genes identified four overexpressed genes with functions related to adhesion. Together with the concomitant overexpression of *uspF* (Table S1A) and underexpression of *ompX* (Table S1B), both located on the chromosome, these observations support that bacterial motility is reduced in the colon (Nachin et al., 2005; Otto et al., 2001). Beyond the specificities linked to this particular enteropathogenic strain of *E. coli*, which would deserve further

investigations, our data are congruent with similar studies using comparative transcriptomics between *in vitro* and *in vivo* conditions for intestinal bacteria (Denou et al., 2007).

The untargeted approach (whole intestinal sections) used for this work has some limitations despite its success for identifying genes involved in phage susceptibility. For instance, the transcriptomic profiles were treated as belonging to a single homogeneous bacterial population, whereas bacteria within an intestinal section actually face different physiological conditions (Li et al., 2015). Moreover, about 50% of the candidate genes identified had no predicted functions. Some may then encode proteins involved in phage-bacterium interactions, warranting additional studies to determine their mode of action.

We showed that four of the genes identified from transcriptomic comparisons alter the interactions of strain 55989 with at least one of the three phages, CLB_P1, CLB_P2 or CLB_P3. When overexpressed or deleted, these genes led to phenotypes that could be related to a global response protecting cells against phages. However, the elicited response was specific to each of the three phages (only 55989Δ*rfaL* cells for CLB_P1, both 55989p*bssR* and 55989p*lsrC* cells for CLB_P2 and both 55989Δ*fliA* and 55989Δ*rfaL* cells for CLB_P3), highlighting the complexity of predicting the *in vivo* efficacy of phages from *in vitro* experiments.

In *E. coli*, LPS is one of the receptors most frequently used by phages (Hantke, 2020). However, as K12 strains (the most frequently used in laboratories) do not synthesise O-antigen (Liu and Reeves, 1994), *rfaL* (the gene encoding the O-antigen ligase) has not previously been identified as a gene involved in phage infection including a recent systematic study (Maffei et al., 2021). Here we demonstrated that phage CLB_P1 recognizes the O104 antigen as a receptor, consistent with its host range towards the ECOR collection (Maura *et al.*, 2012b). Interestingly, the lack of *rfaL* does not completely abolish the capacity of phage CLB_P1 to form plaques on the 55989Δ*rfaL* lawns, suggesting that CLB_P1 recognizes a secondary receptor. However, neither in liquid broth with agitation nor in gut homogenates this secondary receptor was sufficient to allow phage CLB_P1 infection. Therefore, the low rates of replication of phage CLB_P1 on cells in the stationary phase or

364 in colon samples (Fig. 1) can be attributed to the underexpression of *rfaL* identified during the
365 comparative analysis of transcriptomics data. More broadly, when considering application in human,
366 our data suggest that a phage that displays a 3-log reduction of the EOP on a clinical isolate would
367 likely be inefficient *in vivo*.
368 The strong stimulation of biofilm formation by the CLB_P3 phage in the 55989Δ*fliA* and 55989Δ*rfaL*
369 strains was both striking and puzzling, as the functions of these genes are unrelated to each other.
370 Furthermore, these two strains remained as susceptible to CLB_P3 as the WT on both solid and liquid
371 media. It is therefore tempting to speculate that the presence of CLB_P3 led to an increase in the
372 production of an extracellular polysaccharide matrix in these two mutant strains but not in the wild-
373 type, perhaps as a defence against phage CLB_P3. Since *fliA* is a sigma factor, we hypothesize that its
374 absence unlocks a genetic regulation that is otherwise inactive, only in the presence of phage CLB_P3
375 but not of CLB_P1 or CLB_P2. As the lack of *rfaL* affects the structure of the LPS, we hypothesize that
376 the presence of CLB_P3, but not of CLB_P1 or CLB_P2, uncovers a bacterial receptor not involved in
377 phage infection but instead in a signalling process promoting matrix production, perhaps as a phage
378 defence system. Interestingly, these two hypotheses are not exclusive.
379 The presence of phage CLB_P2 increased the formation of biofilms by strains overexpressing either
380 *bssR* or *lsrC* with a similar amplitude. Again, it is tempting to suggest that the increase in biofilm
381 formation is linked to the induction of a phage defence mechanism, as exopolysaccharide production
382 has been shown to protect cells from phage infection in many bacterial species (Darch et al., 2017; de
383 Sousa et al., 2020; Radke and Siegel, 1971). It is worth noting that the presence of CLB_P2, compared
384 to its absence, resulted in the recovery of significantly fewer cells from biofilm for all strains tested.
385 This observation suggests that CLB_P2 may be the most potent of the three phages at killing cells
386 embedded in biofilms. Alternatively, this phage may have a loose affinity for the biofilm matrix (Barr
387 et al., 2013) and decrease the number of CFUs at the plating step instead of within the biofilm.
388 The phenotypes observed with the four genes converged to lower bacterial susceptibility to phages,
389 in other words increasing phage resistance, in both the presence (*in vitro*) and absence (*in vivo*) of

390 phages. This suggests that bacteria become less susceptible to phages when they colonize the gut.
391 Here, the formation of biofilms at the surface of epithelial cells could be invoked as a phage-defence
392 response that could have a negative impact on health when such biofilms are linked to virulence as
393 for the enteroaggregative strain 55989. Moreover, gene regulation entails a lesser fitness cost than
394 loss-of-function due to genetic mutations, which may be crucial to ensure persistence within a
395 fluctuating environment including the competition between bacteria.
396 Experiments in animals with a cocktail of these three phages, or other phage cocktails, have shown
397 that despite initially reduction of bacterial levels in the gut, coexistence of phages with their hosts is
398 rapidly established (Hsu et al., 2019; Maura *et al.*, 2012b). This coexistence is supported by multiple
399 overlapping mechanisms, including the regulation of bacterial gene expression, as shown here
400 (Javaudin et al., 2021; Lourenço *et al.*, 2018). Aligning the composition of phage cocktails to the
401 environmental conditions in which they are to be used, may be the best option for optimizing phage
402 applications. In addition, repeated phage applications, prescribed like a standard anti-microbial drug,
403 might result in more effective treatments by preventing the establishment of coexistence.
404 In conclusion, tripartite interactions occur between phages, bacteria and the host, all of which
405 influence each other. The mammalian gut environment and its response to bacterial colonisation
406 affects bacterial gene expression, which in turns influences phage infection. Conversely, phage
407 variants may be selected to improve efficacy against established bacterial clones by adaptation (De
408 Sordi et al., 2017; Mathieu et al., 2020), potentially inducing a response in the bacteria (De Sordi *et*
409 *al.*, 2019) affecting their relationship with the host (intestinal epithelial and immune cells) (Diard et
410 al., 2017; Sausset et al., 2020). Globally, the balance between these equilibria governs gut
411 homeostasis and health.

Acknowledgements

We thank Jorge Moura de Sousa for writing the customised R script for the pairwise comparisons between lists of genes from the different samples and for critically reading the manuscript. We thank Dwayne Roach and Anne Chevallereau for valuable discussions. We thank the Genetics of Biofilms team (Jean-Marc Ghigo) of Institut Pasteur and in particular Anne-Aurélie Lopes for training on the biofilm assays and Christophe Beloin for access to the ASKA plasmids collection. We thank the members of the Centre for Gnotobiology Platform of the Institut Pasteur (Thierry Angélique, Eddie Maranghi, Martine Jacob, Jérome Toutain and Marisa Gabriela Lopez Dieguez) for their help with the animal work. ML is funded as part of the Pasteur - Paris University (PPU) International PhD Program. ML is funded by Institut Carnot Pasteur Maladies Infectieuses (ANR 11-CARN 017-01). LDS is funded by a Roux-Cantarini fellowship from the Institut Pasteur (Paris, France). LC is funded by a PhD fellowship from the Ministère de l'Enseignement Supérieur et de la Recherche, France, Ecole Doctorale 394. QLB is funded by École Doctorale FIRE - Programme Bettencourt. MT received a fellowship from Fondation DigestScience. The Transcriptome and Epigenome Platform is part of the France Génomique consortium (ANR10-NBS-09-08).

Author contributions

Conceptualization and Methodology, L.D., L.D.S. and M.L. Investigations, L.C., M.L., M.T., O.S., Q.L.B. and T.P. Formal analysis, J.Y.C., R.L., M.L. and H.V. Resources, MB. Supervision and Funding Acquisition L.D. Writing - Original Draft, M.L. and L.D. Writing – Review and Editing, L.C., L.D., L.D.S., Q.L.B., M.L. and T.P.

Declaration of interest

None to declare

Main figure titles and legends

Figure 1. The replication of phages CLB_P1, CLB_P2 and CLB_P3 on strain 55989 is affected by growth conditions *in vitro* and *ex vivo*

Phages CLB_P1, CLB_P2 or CLB_P3 were added to LB (green) or to homogenized gut sections (ile, ileum, dark blue; col, colon, light blue) from axenic mice and incubated during 5 h before quantification (left part). The amplification of phages (CLB_P1, CLB_P2, CLB_P3, each added at an MOI of approximately 0.01) is reported after 5 h of incubation with strain 55989 (central part) in the indicated conditions: exponentially growing cells (exp, dark green; OD_{600}=0.5); cells in stationary phase (sta, light green; equivalent OD_{600}=5); homogenized gut sections from monocolonized mice (ile, ileum, dark blue; col, colon, light blue). 55989 cells collected from exponential or stationary growth conditions were incubated with homogenized gut sections from axenic mice during 5 h and their density was reported (right part). Median n-fold multiplication is shown relative to the initial number of plaque-forming units (PFUs) or colony-forming units (CFUs). n=2 to 5 biological replicates with 1 to 3 technical replicates.

Figure 2. The mRNA content of *E. coli* cells growing in the gut is different from that of cells grown *in vitro*

A. Cells of *E. coli* strain 55989 were collected from *in vitro* cultures (LB medium, 37°C with shaking) at an OD_{600nm} of 0.5 (exponential, *n*=4) and an equivalent OD_{600nm} of 5 (stationary, *n*=4) or from *in vivo* tissues (colon of monocolonized mice, *n*=4) and their mRNA was extracted, sequenced and subjected to principal component analysis (biological variability was the main source of variance). **B.** Heatmap and dendrogram obtained for VST-transformed data for sequenced mRNAs from the samples analysed in A (see methods). **C.** Numbers of overexpressed (O/E) and underexpressed (U/E) genes from pairwise comparisons between colon and either exponential or stationary phase samples. **D.** Numbers of overexpressed (O/E) and underexpressed (U/E) genes from pairwise comparisons between exponential and either stationary or colon samples.

Figure 3. The growth of *E. coli* strain 55989 in the colon involves the activation of carbohydrate metabolism and a decrease in aerobic respiration

A network analysis was performed, based on translated protein–protein interactions, with the STRING webserver (string-db.org) using strain MG1655 as template, on genes overexpressed (**A**) and underexpressed (**B**) in the colon of monocolonized mice relative to cells in the stationary and exponential growth phases. The full list of genes analysed is available in Tables S1 and S2. The large closed circles (orange for overexpressed and blue for underexpressed genes) correspond to pathways indicated in bold and discussed in the text.

Figure 4. Phage CLB_P1 does not infect 55989Δ*rfaL* cells and recognizes the O104-antigen moiety of the LPS.

A. Growth curves in LB of the *E. coli* strains 55989 (WT), 55989Δ*rfaL* and 55989Δ*fliA* (supplemented with kanamycin for Δ*rfaL* and Δ*fliA* strains), in the presence and absence of phage CLB_P1, added at *t*=0, at an MOI of 0.01 (*n*=2 to 3 for each set of conditions). Error = standard error of the mean.

B. Growth curves in LB of *E. coli* strain 55989 (WT), WT+p*bssR* (supplemented with 0.05 mM IPTG) and WT+p*lsrC* (supplemented with 0.01 mM IPTG) in presence or absence of phage CLB_P1 added at *t*=0 and a MOI of 0.01 (*n*=2 to 3 for each condition). Errors = standard error of the mean.

C, D, E. The adsorption of phage CLB_P1 on strains 55989Δ*rfaL* (C), 55989 (D) and 55989Δ*fliA* (E) was evaluated according to standard procedures (see methods). Adsorption constants and adsorption kinetics (90% of phages bound) were calculated by applying an exponential decay function to the corresponding data.

F. Microscopic observations of 55989 cells ($1x10^7$ CFU) mixed with either PBS or phage CLB_P1 ($2.5x10^7$ PFU) or a *Pseudomonas aeruginosa* phage ($2.5x10^7$ PFU) during 10 min, followed by the addition of either O104 anti-serum or PBS. Scale bar, 20 µm

Figure 5. Phage CLB_P2 increases the formation of biofilms in 55989 cells overexpressing either *bssR* or *lsrC* genes.

A. Growth curves in LB of *E. coli* strain 55989 (WT), WT+p*bssR* (supplemented with 0.05 mM IPTG) and WT+p*lsrC* (supplemented with 0.01 mM IPTG) in presence or absence of phage CLB_P2 added at *t*=0 and a MOI of 0.01 (*n*=2 to 3 for each condition). Errors = standard error of the mean.

B. Growth curves in LB of the *E. coli* strains 55989 (WT), 55989Δ*rfaL* and 55989Δ*fliA* (supplemented with kanamycin for Δ*rfaL* and Δ*fliA* strains), in the presence and absence of phage CLB_P2, added at *t*=0, at an MOI of 0.01 (*n*=2 to 3 for each set of conditions). Error = standard error of the mean.

C. Biofilm formation, reported as variations of OD_{570nm} recorded at 48 h relative to 24 h for the indicated *E. coli* strains in the presence or absence of phage CLB_P2 added at 24 h ($1x10^7$ PFU/mL) and IPTG at 0.05 mM for empty and *bssR* plasmids or 0.01 mM for the *lsrC* plasmid, as well as kanamycin; *n*=3 to 4 independent experiments. The boxes indicate the interquartile range; the horizontal bars correspond to the median and the vertical bars indicated the minimum and maximum values (within 1.5 interquartile intervals), *p*=*p*-value of the Tukey post-hoc tests (Table S2A).

D. Number of CFU resuspended from biofilms recovered from microplates set up in parallel to those used for biofilm quantification shown in panel C (see methods).

Figure 6. Phage CLB_P3 increases biofilms formation in 55989 cells deleted for either *fliA* or *rfaL* genes.

A. Growth curves in LB of *E. coli* strain 55989 (WT), WT+p*bssR* (supplemented with 0.05 mM IPTG) and WT+p*lsrC* (supplemented with 0.01 mM IPTG) in presence or absence of phage CLB_P3 added at *t*=0 and a MOI of 0.01 (*n*=2 to 3 for each condition). Errors = standard error of the mean.

B. Growth curves in LB of the *E. coli* strains 55989 (WT), 55989Δ*rfaL* and 55989Δ*fliA* (supplemented with kanamycin for Δ*rfaL* and Δ*fliA* strains), in the presence and absence of phage CLB_P3, added at *t*=0, at an MOI of 0.01 (*n*=2 to 3 for each set of conditions). Errors = standard error of the mean.

C. Biofilm formation, reported as change in OD_{570nm} at 48 h relative to 24 h for the indicated *E. coli* strains in the presence or absence of phage CLB_P3 added at 24 h ($1x10^7$ PFU/mL); *n*=3 to 4 independent experiments. When necessary IPTG was added at 0.05 mM. The boxes represent the interquartile range; the horizontal bars represent the median and the vertical bars represent the minimum and maximum values (within 1.5 interquartile intervals), *p*=*p*-value for post hoc Tukey tests (Table S2A).

D. Number of CFU resuspended from biofilms recovered from microplates set up in parallel with those used to quantify biofilms shown in panel C (see methods).

Figure 7. Phage CLB_P1 cannot replicate on intestinal homogenates of 55989Δ*rfaL*-colonized mice. Amplification (*n*=2 biological replicates) of phages (CLB_P1, CLB_P2, CLB_P3, each added at an MOI of approximately 0.01) after 5 hours of incubation with either strain 55989Δ*rfaL* or 55989Δ*fliA* from homogenized gut sections from either 55989Δ*rfaL*- or 55989Δ*fliA*-monocolonized mice (ile, ileum, dark blue; col, colon, light blue). The median n-fold multiplication is shown relative to the initial number of PFUs or CFUs.

STAR Methods

Resource Availability

Lead Contact

Further information and requests for resources and reagents should be directed to and will be fulfilled by the lead contact, Laurent Debarbieux (laurent.debarbieux@pasteur.fr).

Materials Availability

The bacterial strains 55989Δ*rfaL* and 55989Δ*fliA* as well as phages are available from the lead contact upon completion of a Materials Transfer Agreement (MTA).

Data and Code Availability.

RNA-Seq data have been deposited at GEO and are publicly available as of the date of publication. Accession numbers are listed in the key resources table.

This paper does not report original code.

Any additional information required to reanalyze the data reported in this paper is available from the lead contact upon request.

Experimental models and subject details

Ethics statement

C3H axenic mice (seven to nine weeks old) reared at Institut Pasteur (Paris, France) were housed in an animal facility in accordance with Institut Pasteur guidelines and European recommendations. Food and drinking water were provided *ad libitum*. Protocols were approved by the veterinary staff of the Institut Pasteur animal facility (Ref.#18.271) and the National Ethics Committee (APAFIS#26874-2020081309052574 v1). We used 17 mice (15 males and 2 female) for this study.

Phages and bacterial strains

The *Escherichia coli* strain 55989 was previously described (Mossoro et al., 2002) and other strains are listed in the key resources table.

Phages CLB_P1 (KC109329.1), CLB_P2 (OL770107) and CLB_P3 (OL770108) have been described elsewhere (Maura *et al.*, 2012b). The 55989 mutants were obtained by a three-step PCR in which each gene (*rfaL and fliA*) was disrupted by the insertion of a kanamycin resistance marker gene by lambda Red-mediated homologous recombination (Chaveroche et al., 2000). Primers used for this study are listed in key resources table. ASKA plasmids (chloramphenicol resistant) were used for the overexpression of *bssR* and *lsrC* and the complementation of 55989Δ*rfaL* and 55989Δ*fliA* strains (Kitagawa et al., 2005).

Strains were routinely cultured in lysogeny broth (LB Lennox - BD), or on LB Lennox agar (BD) or Drigalski agar (lactose agar with bromothymol blue and crystal violet- CONDA) plates, at 37ºC. When required for selection, streptomycin (100 µg/mL) or kanamycin (100 µg/mL) or chloramphenicol (30 µg/ml) (Sigma) was added.

Methods details

***Ex vivo* assay**

C3H axenic mice received 200 µL of PBS or strains 55989 or 55989Δ*fliA* or 55989Δ*rfaL* (10^7 CFU prepared from an overnight culture in LB at 37°C) in sterile sucrose sodium bicarbonate solution (20% sucrose and 2.6% sodium bicarbonate, pH 8) by oral gavage. Three days later, they were killed, and intestinal sections (ileum and colon) were collected and weighed. PBS was added to each sample (1.75 mL for ileum and colon) before homogenisation (Oligo-Macs, Miltenyi Biotec). We dispensed 140 µL of each homogenized sample into the wells of a 96-well plate and 10 µL of each individual phage was added, to reach an MOI of 1 x 10^{-2}, and the plate was incubated at 37°C. A fraction of the homogenized samples was also serially diluted in PBS and plated on Drigalski medium for the counting of *E. coli* colonies at *t*=0. Following five hours of incubation, samples were serially diluted in

PBS and plated on Drigalski medium and on LB agar plates overlaid with strain 55989. Both sets of plates were incubated at 37°C overnight. The same procedure was followed for *in vitro* assays with bacteria collected during the exponential (OD_{600}=0.5) or stationary (24 h; equivalent OD_{600}=5) growth phases, at 37°C, with shaking. These cells were also incubated during 5 h with homogenized gut samples from axenic mice as a control of experiments performed with samples from monocolonized mice.

Transcriptomics

Strain 55989 was grown overnight at 37°C with shaking (n=4 replicates). Cultures were diluted in fresh medium and incubated until they reached an OD_{600nm} of about 0.5, at which point, half the volume was collected for RNA extraction, the other half being maintained at 37°C, with shaking, up to 24 h at which time point they reached an equivalent OD_{600nm} of 5, corresponding to stationary phase. RNA was extracted by centrifuging the cells and incubating them with TRIzol (Sigma T-9424) for lysis.

For intestinal samples, axenic mice received 200 µL of strain 55989 (10^7 CFU prepared from an overnight culture in LB at 37°C) in sterile sucrose sodium bicarbonate solution (20% sucrose and 2.6% sodium bicarbonate, pH 8) by oral gavage. Three days later, the mice were killed, and intestinal sections were collected and immediately frozen in liquid nitrogen (ileum and colon). TRIzol was then added to the frozen samples, which were homogenized (Oligo-Macs, Miltenyi Biotec). Total RNA from both *in vitro* and *in vivo* samples was purified by standard organic extraction (phenol/chloroform) followed by ethanol precipitation. It was then treated with the RNeasy mini kit (Qiagen) for final purification, and the remaining genomic DNA was removed with an on-column RNAse-free DNAse set protocol (Qiagen). RNA integrity was assessed with the Bioanalyser system (Agilent) and RNA integrity number (RIN) and ribosomal ratio (23S/16S) were determined. We obtained rRNA-depleted RNA with the Ribo-Zero rRNA depletion kit for eukaryotic and prokaryotic RNA (Illumina). Libraries were prepared with the TruSeq Stranded RNA LT prep kit (Illumina), with

final validation on the Bioanalyser system. Final DNA quantification was performed with sensitive fluorescence-based quantification assays ("Quant-It" assay kit and a QuBit fluorometer, Invitrogen). Librairies were then normalised to a concentration of 2 nM and multiplexed. The samples were then denatured at a concentration of 1 nM with 0.1 N NaOH at room temperature, and were finally diluted to 9.5 pM for loading onto the sequencing flowcell. Sequencing was performed on an Illumina HiSeq 2500 machine, producing 65 bp single-reads. A mean of 266 M and 2 M of reads was obtained for colonic and in vitro samples, respectively.

Data analysis

After sequencing, we performed a first quality check with fastQC (https://www.bioinformatics.babraham.ac.uk/projects/fastqc/), and then cleaned up the reads with cutadapt (Martin, 2011). Bowtie was used for read alignment and files were transformed into BAM and SAM formats with samtools software (Li et al., 2009). Finally, reads were counted with featureCounts and the statistical analysis was performed with R software (https://www.r-project.org/)(Gentleman et al., 2004) packages including DESeq2 (Anders and Huber, 2010; Love et al., 2014) and the SARTools package (Varet et al., 2016). Normalisation and differential analysis were performed with the DESeq2 model and package. This report comes with additional tab-delimited text files containing lists of differentially expressed features. A gene ontology analysis was performed on the lists of under- and overexpressed genes (http://geneontology.org/). Gene functions were verified with the EcoCyc database (Keseler *et al.*, 2011). A comparative analysis was performed with a customised R script performing all possible pairwise comparisons between the gene lists for the different samples. A variance stabilizing transformation (VST) representation of the data was obtained with the DESeq2 package (Love *et al.*, 2014). Protein-protein association networks were generated with the STRING webserver (https://string-db.org/network/) using the MG1655 strain as a template (Szklarczyk et al., 2019). Putative prophages in the *E. coli* 55989 genome were identified using PHASTER (PHAge Search Tool - Enhanced Release) (Arndt et al., 2016) and are listed below.

prediction	start	end	size (kb)
questionable	821138	866847	45.7
intact	1093207	1140290	45.0
incomplete	1408037	1417268	9.2
intact	1420060	1456075	36.0
intact	1758317	1808332	50.0
intact	2141235	2180631	39.3
intact	2664274	2710113	45.8
intact	3339788	3384869	45.0
intact	4784434	4810665	26.2

634

635

636 **Phage efficiency of plating (EOP) test**

637 The efficiency of plating (EOP) was calculated (ratio of the number of plaques formed by the phage
638 on each strain tested to the number of plaques formed on the host strain 55989) for each phage.
639 Three independent replicates were performed using bacterial cultures grown to an OD of
640 approximately 0.2 and spread on LB plates onto which phage dilutions were spotted. Plates were
641 incubated at 37°C overnight.

642

643 **Adsorption assays and phage growth**

644 Three independent adsorption assays were performed for each phage, in accordance with a
645 previously described protocol (Chevallereau et al., 2016). Data were approximated with an
646 exponential decay function and adsorption times were defined as the time required to reach a
647 threshold of 10% non-adsorbed phage particles. Phage growth and bacterial lysis were assessed by
648 diluting an overnight culture of each strain in LB broth and culturing the cells to an OD_{600nm} of 0.2. We
649 then dispensed 140 µL of this culture into each of the wells of a 96-well plate (Microtest 96 plates,

Falcon). We added 10 µL of sterile phage lysate diluted in PBS to obtain a multiplicity of infection (MOI) of 1 x 10^{-2} to each well. Plates were incubated in a microplate reader at 37°C, with shaking 30 s before the automatic recording of OD_{600nm} at 15-minute intervals over a period of 20 hours (GloMax®-Multi Detection System, Promega, USA).

Biofilm formation and quantification

Overnight bacterial cultures were diluted 1:100 in LB medium with, when required, chloramphenicol or kanamycin, and dispensed into UV-sterilised 96-well PVC microplates. The wells located at the edge of the microplates were filled with 200 µL water to prevent evaporation during incubation in a static chamber, at 37°C, for 24 h and 48 h. Two microplates were used after 24 h, for biofilm staining and CFU counts. Biofilm staining was performed by adding 125 µL of 1% crystal violet (V5265; Sigma-Aldrich) to wells previously washed twice with water. After 15 minutes of staining, the crystal violet solution was removed by flicking, and biofilms were washed three times with water. For CFU counts, aggregates were homogenized within the wells by repeated pipetting and serial dilutions were plated on LB agar plates. For the other eight microplates, the LB medium was removed at 24 h by pipetting. Two microplates were filled with LB and incubated for a further 24 h and the treated as described above for the 24 h time point. A similar pair of microplates was filled with one of the three phages ($2x10^6$ PFU in 200 µL in LB) and incubated for a further 24 h. These microplates were treated as described above for the 24 h time point. Stained microplates were left to dry overnight under a hood and the crystal violet was then resuspended in a 1:4 acetone:ethanol mixture, for the reading of absorbance at 570 nm (Tecan Infinite M200 PRO). For each microplate, we measured the OD for five technical replicates (five wells), and three to five independent experiments were performed for each strain.

Agglutination assay

675 The O104 immun-serum (Monospecific O Rabbit antiserum, réf #45840, lot O104L11H11, SSI
676 Diagnostica) was used as recommended by the provider. Briefly, a volume of 700 µL of a stationary
677 phase liquid culture of strain 55989 grown in LB at 37°C under agitation was centrifuged 10 min at
678 5.000g and after discarding the supernatant, the pellet was resuspended in 700 µL of PBS. This
679 sample was heated during 80 minutes at 99°C and then cooled to room temperature as
680 recommended. Then 5 µL ($1x10^7$ CFU) of this sample was introduce in different wells of a96-well
681 plates (Microtest 96 plates, Falcon). Then either 5 µL of PBS, or phage CLB_P1 ($2.5.10^7$ PFU) or phage
682 PAK_P3 ($2.5.10^7$ PFU). After 10 minutes at room temperature either 10 µL of PBS or O104 immun-
683 serum was added and the plate was incubated 1 h at 37°C. Next, a drop (5 µL) of each condition was
684 put on a glass slide and covered with a cover slip for direct examination under a phase contrast
685 microscope (Olympus IX81). Pictures were taken at X20 magnification.
686

687 ## Quantification and statistical analysis

688 Quantification and statistical analysis of the transcriptomics data are reported in the corresponding
689 Methods section and in the Table S1.
690 For the growth curves of bacterial strains (n=2 to 3 for each condition) error bars represent standard
691 error of the mean (SEM) as indicate in the legends of Figures 4, 5 and 6. Statistical analysis on the
692 number of bacteria and the OD570nm generated by the biofilm experiments were carried out using
693 the lme4, lmerTest and car packages of R (Bates et al., 2015; Fox and Weisberg, 2018; Kuznetsova et
694 al., 2017). CFU were log10-transformed prior to analysis. Linear mixed-models were used to account
695 for random experimental effects (i.e. the effect of the plate and experiments). Prior analysis,
696 normality was assessed with a QQ-plot. Overall effects were assessed with Analysis of Variance
697 (ANOVA) and post-hoc Tukey's comparisons and were performed using the lsmeans R package
698 (Lenth, 2016). $p< 0.05$ was considered statistically significant. The results of the comparisons are
699 recapitulated in Table S2A and S2B.
700

Declaration of Interests

The authors declare no competing interests.

References

Alseth, E.O., Pursey, E., Luján, A.M., McLeod, I., Rollie, C., and Westra, E.R. (2019). Bacterial biodiversity drives the evolution of CRISPR-based phage resistance. Nature *574*, 549-552. 10.1038/s41586-019-1662-9.

Anders, S., and Huber, W. (2010). Differential expression analysis for sequence count data. Genome biology *11*, R106. 10.1186/gb-2010-11-10-r106.

Arndt, D., Grant, J.R., Marcu, A., Sajed, T., Pon, A., Liang, Y., and Wishart, D.S. (2016). PHASTER: a better, faster version of the PHAST phage search tool. Nucleic acids research *44*, W16-21. 10.1093/nar/gkw387.

Barr, J.J., Auro, R., Furlan, M., Whiteson, K.L., Erb, M.L., Pogliano, J., Stotland, A., Wolkowicz, R., Cutting, A.S., Doran, K.S., et al. (2013). Bacteriophage adhering to mucus provide a non-host-derived immunity. Proceedings of the National Academy of Sciences of the United States of America *110*, 10771-10776. 10.1073/pnas.1305923110.

Barroso-Batista, J., Sousa, A., Lourenço, M., Bergman, M.L., Sobral, D., Demengeot, J., Xavier, K.B., and Gordo, I. (2014). The first steps of adaptation of Escherichia coli to the gut are dominated by soft sweeps. PLoS genetics *10*, e1004182. 10.1371/journal.pgen.1004182.

Bates, D., Mächler, M., Bolker, B., and Walker, S. (2015). Fitting Linear Mixed-Effects Models Using lme4. Journal of Statistical Software *67*, 1 - 48. 10.18637/jss.v067.i01.

Bernheim, A., and Sorek, R. (2020). The pan-immune system of bacteria: antiviral defence as a community resource. Nature reviews. Microbiology *18*, 113-119. 10.1038/s41579-019-0278-2.

Bertin, Y., Girardeau, J.P., Chaucheyras-Durand, F., Lyan, B., Pujos-Guillot, E., Harel, J., and Martin, C. (2011). Enterohaemorrhagic Escherichia coli gains a competitive advantage by using ethanolamine as a nitrogen source in the bovine intestinal content. Environmental microbiology *13*, 365-377. 10.1111/j.1462-2920.2010.02334.x.

Boll, E.J., Ayala-Lujan, J., Szabady, R.L., Louissaint, C., Smith, R.Z., Krogfelt, K.A., Nataro, J.P., Ruiz-Perez, F., and McCormick, B.A. (2017). Enteroaggregative Escherichia coli Adherence Fimbriae Drive Inflammatory Cell Recruitment via Interactions with Epithelial MUC1. mBio *8*. 10.1128/mBio.00717-17.

Bull, J.J., Vegge, C.S., Schmerer, M., Chaudhry, W.N., and Levin, B.R. (2014). Phenotypic resistance and the dynamics of bacterial escape from phage control. PloS one *9*, e94690. 10.1371/journal.pone.0094690.

Chapman-McQuiston, E., and Wu, X.L. (2008). Stochastic receptor expression allows sensitive bacteria to evade phage attack. Part I: experiments. Biophysical journal *94*, 4525-4536. 10.1529/biophysj.107.120212.

Chaudhry, W.N., Pleška, M., Shah, N.N., Weiss, H., McCall, I.C., Meyer, J.R., Gupta, A., Guet, C.C., and Levin, B.R. (2018). Leaky resistance and the conditions for the existence of lytic bacteriophage. PLoS biology *16*, e2005971. 10.1371/journal.pbio.2005971.

Chaveroche, M.K., Ghigo, J.M., and d'Enfert, C. (2000). A rapid method for efficient gene replacement in the filamentous fungus Aspergillus nidulans. Nucleic acids research *28*, E97. 10.1093/nar/28.22.e97.

Chevallereau, A., Blasdel, B.G., De Smet, J., Monot, M., Zimmermann, M., Kogadeeva, M., Sauer, U., Jorth, P., Whiteley, M., Debarbieux, L., and Lavigne, R. (2016). Next-Generation "-omics" Approaches Reveal a Massive Alteration of Host RNA Metabolism during Bacteriophage Infection of Pseudomonas aeruginosa. PLoS genetics *12*, e1006134. 10.1371/journal.pgen.1006134.

748 Choi, Y., Shin, H., Lee, J.H., and Ryu, S. (2013). Identification and characterization of a novel flagellum-
749 dependent Salmonella-infecting bacteriophage, iEPS5. Applied and environmental microbiology *79*,
750 4829-4837. 10.1128/aem.00706-13.
751 Condon, C., and Weiner, J.H. (1988). Fumarate reductase of Escherichia coli: an investigation of
752 function and assembly using in vivo complementation. Molecular microbiology *2*, 43-52.
753 10.1111/j.1365-2958.1988.tb00005.x.
754 Conway, T., and Cohen, P.S. (2015). Commensal and Pathogenic Escherichia coli Metabolism in the
755 Gut. Microbiology spectrum *3*. 10.1128/microbiolspec.MBP-0006-2014.
756 Cornuault, J.K., Moncaut, E., Loux, V., Mathieu, A., Sokol, H., Petit, M.A., and De Paepe, M. (2020).
757 The enemy from within: a prophage of Roseburia intestinalis systematically turns lytic in the mouse
758 gut, driving bacterial adaptation by CRISPR spacer acquisition. The ISME journal *14*, 771-787.
759 10.1038/s41396-019-0566-x.
760 Cotter, P.A., Chepuri, V., Gennis, R.B., and Gunsalus, R.P. (1990). Cytochrome o (cyoABCDE) and d
761 (cydAB) oxidase gene expression in Escherichia coli is regulated by oxygen, pH, and the fnr gene
762 product. Journal of bacteriology *172*, 6333-6338. 10.1128/jb.172.11.6333-6338.1990.
763 Croxen, M.A., and Finlay, B.B. (2010). Molecular mechanisms of Escherichia coli pathogenicity.
764 Nature reviews. Microbiology *8*, 26-38. 10.1038/nrmicro2265.
765 Darch, S.E., Kragh, K.N., Abbott, E.A., Bjarnsholt, T., Bull, J.J., and Whiteley, M. (2017). Phage Inhibit
766 Pathogen Dissemination by Targeting Bacterial Migrants in a Chronic Infection Model. mBio *8*.
767 10.1128/mBio.00240-17.
768 De Sordi, L., Khanna, V., and Debarbieux, L. (2017). The Gut Microbiota Facilitates Drifts in the
769 Genetic Diversity and Infectivity of Bacterial Viruses. Cell host & microbe *22*, 801-808.e803.
770 10.1016/j.chom.2017.10.010.
771 De Sordi, L., Lourenço, M., and Debarbieux, L. (2019). "I will survive": A tale of bacteriophage-
772 bacteria coevolution in the gut. Gut microbes *10*, 92-99. 10.1080/19490976.2018.1474322.
773 de Sousa, J.A.M., Buffet, A., Haudiquet, M., Rocha, E.P.C., and Rendueles, O. (2020). Modular
774 prophage interactions driven by capsule serotype select for capsule loss under phage predation. The
775 ISME journal *14*, 2980-2996. 10.1038/s41396-020-0726-z.
776 Denou, E., Berger, B., Barretto, C., Panoff, J.M., Arigoni, F., and Brüssow, H. (2007). Gene expression
777 of commensal Lactobacillus johnsonii strain NCC533 during in vitro growth and in the murine gut.
778 Journal of bacteriology *189*, 8109-8119. 10.1128/jb.00991-07.
779 Deriu, E., Liu, J.Z., Pezeshki, M., Edwards, R.A., Ochoa, R.J., Contreras, H., Libby, S.J., Fang, F.C., and
780 Raffatellu, M. (2013). Probiotic bacteria reduce salmonella typhimurium intestinal colonization by
781 competing for iron. Cell host & microbe *14*, 26-37. 10.1016/j.chom.2013.06.007.
782 Diard, M., Bakkeren, E., Cornuault, J.K., Moor, K., Hausmann, A., Sellin, M.E., Loverdo, C., Aertsen, A.,
783 Ackermann, M., De Paepe, M., et al. (2017). Inflammation boosts bacteriophage transfer between
784 Salmonella spp. Science (New York, N.Y.) *355*, 1211-1215. 10.1126/science.aaf8451.
785 Domka, J., Lee, J., and Wood, T.K. (2006). YliH (BssR) and YceP (BssS) regulate Escherichia coli K-12
786 biofilm formation by influencing cell signaling. Applied and environmental microbiology *72*, 2449-
787 2459. 10.1128/aem.72.4.2449-2459.2006.
788 Fabich, A.J., Jones, S.A., Chowdhury, F.Z., Cernosek, A., Anderson, A., Smalley, D., McHargue, J.W.,
789 Hightower, G.A., Smith, J.T., Autieri, S.M., et al. (2008). Comparison of carbon nutrition for
790 pathogenic and commensal Escherichia coli strains in the mouse intestine. Infection and immunity
791 *76*, 1143-1152. 10.1128/iai.01386-07.
792 Fajardo, D.A., Cheung, J., Ito, C., Sugawara, E., Nikaido, H., and Misra, R. (1998). Biochemistry and
793 regulation of a novel Escherichia coli K-12 porin protein, OmpG, which produces unusually large
794 channels. Journal of bacteriology *180*, 4452-4459. 10.1128/jb.180.17.4452-4459.1998.
795 Feugeas, J.P., Tourret, J., Launay, A., Bouvet, O., Hoede, C., Denamur, E., and Tenaillon, O. (2016).
796 Links between Transcription, Environmental Adaptation and Gene Variability in Escherichia coli:
797 Correlations between Gene Expression and Gene Variability Reflect Growth Efficiencies. Molecular
798 biology and evolution *33*, 2515-2529. 10.1093/molbev/msw105.
799 Fox, J., and Weisberg, S. (2018). An R Companion to Applied Regression (SAGE Publications).

Galtier, M., De Sordi, L., Sivignon, A., de Vallée, A., Maura, D., Neut, C., Rahmouni, O., Wannerberger, K., Darfeuille-Michaud, A., Desreumaux, P., et al. (2017). Bacteriophages Targeting Adherent Invasive Escherichia coli Strains as a Promising New Treatment for Crohn's Disease. Journal of Crohn's & colitis *11*, 840-847. 10.1093/ecco-jcc/jjw224.

Gentleman, R.C., Carey, V.J., Bates, D.M., Bolstad, B., Dettling, M., Dudoit, S., Ellis, B., Gautier, L., Ge, Y., Gentry, J., et al. (2004). Bioconductor: open software development for computational biology and bioinformatics. Genome biology *5*, R80. 10.1186/gb-2004-5-10-r80.

Golec, P., Karczewska-Golec, J., Łoś, M., and Węgrzyn, G. (2014). Bacteriophage T4 can produce progeny virions in extremely slowly growing Escherichia coli host: comparison of a mathematical model with the experimental data. FEMS microbiology letters *351*, 156-161. 10.1111/1574-6968.12372.

Gregory, A.C., Zablocki, O., Zayed, A.A., Howell, A., Bolduc, B., and Sullivan, M.B. (2020). The Gut Virome Database Reveals Age-Dependent Patterns of Virome Diversity in the Human Gut. Cell host & microbe *28*, 724-740.e728. 10.1016/j.chom.2020.08.003.

Hadas, H., Einav, M., Fishov, I., and Zaritsky, A. (1997). Bacteriophage T4 development depends on the physiology of its host Escherichia coli. Microbiology (Reading, England) *143 (Pt 1)*, 179-185. 10.1099/00221287-143-1-179.

Hantke, K. (2020). Compilation of Escherichia coli K-12 outer membrane phage receptors - their function and some historical remarks. FEMS microbiology letters *367*. 10.1093/femsle/fnaa013.

Helmann, J.D., and Chamberlin, M.J. (1987). DNA sequence analysis suggests that expression of flagellar and chemotaxis genes in Escherichia coli and Salmonella typhimurium is controlled by an alternative sigma factor. Proceedings of the National Academy of Sciences of the United States of America *84*, 6422-6424. 10.1073/pnas.84.18.6422.

Hoque, M.M., Naser, I.B., Bari, S.M., Zhu, J., Mekalanos, J.J., and Faruque, S.M. (2016). Quorum Regulated Resistance of Vibrio cholerae against Environmental Bacteriophages. Scientific reports *6*, 37956. 10.1038/srep37956.

Hsu, B.B., Gibson, T.E., Yeliseyev, V., Liu, Q., Lyon, L., Bry, L., Silver, P.A., and Gerber, G.K. (2019). Dynamic Modulation of the Gut Microbiota and Metabolome by Bacteriophages in a Mouse Model. Cell host & microbe *25*, 803-814.e805. 10.1016/j.chom.2019.05.001.

Javaudin, F., Latour, C., Debarbieux, L., and Lamy-Besnier, Q. (2021). Intestinal Bacteriophage Therapy: Looking for Optimal Efficacy. Clin Microbiol Rev *34*, e0013621. 10.1128/CMR.00136-21.

Keseler, I.M., Collado-Vides, J., Santos-Zavaleta, A., Peralta-Gil, M., Gama-Castro, S., Muñiz-Rascado, L., Bonavides-Martinez, C., Paley, S., Krummenacker, M., Altman, T., et al. (2011). EcoCyc: a comprehensive database of Escherichia coli biology. Nucleic acids research *39*, D583-590. 10.1093/nar/gkq1143.

Kirsch, J.M., Brzozowski, R.S., Faith, D., Round, J.L., Secor, P.R., and Duerkop, B.A. (2021). Bacteriophage-Bacteria Interactions in the Gut: From Invertebrates to Mammals. Annu Rev Virol *8*, 95-113. 10.1146/annurev-virology-091919-101238.

Kitagawa, M., Ara, T., Arifuzzaman, M., Ioka-Nakamichi, T., Inamoto, E., Toyonaga, H., and Mori, H. (2005). Complete set of ORF clones of Escherichia coli ASKA library (a complete set of E. coli K-12 ORF archive): unique resources for biological research. DNA research : an international journal for rapid publication of reports on genes and genomes *12*, 291-299. 10.1093/dnares/dsi012.

Klena, J.D., Ashford, R.S., 2nd, and Schnaitman, C.A. (1992). Role of Escherichia coli K-12 rfa genes and the rfp gene of Shigella dysenteriae 1 in generation of lipopolysaccharide core heterogeneity and attachment of O antigen. Journal of bacteriology *174*, 7297-7307. 10.1128/jb.174.22.7297-7307.1992.

Kuznetsova, A., Brockhoff, P.B., and Christensen, R.H.B. (2017). lmerTest Package: Tests in Linear Mixed Effects Models. Journal of Statistical Software *82*, 1 - 26. 10.18637/jss.v082.i13.

Lääveri, T., Antikainen, J., Mero, S., Pakkanen, S.H., Kirveskari, J., Roivainen, M., and Kantele, A. (2020). Bacterial, viral and parasitic pathogens analysed by qPCR: Findings from a prospective study of travellers' diarrhoea. Travel medicine and infectious disease *40*, 101957. 10.1016/j.tmaid.2020.101957.

Labedan, B. (1984). Requirement for a fluid host cell membrane in injection of coliphage T5 DNA. Journal of virology *49*, 273-275. 10.1128/jvi.49.1.273-275.1984.
Labrie, S.J., Samson, J.E., and Moineau, S. (2010). Bacteriophage resistance mechanisms. Nature reviews. Microbiology *8*, 317-327. 10.1038/nrmicro2315.
Lau, C.K., Krewulak, K.D., and Vogel, H.J. (2016). Bacterial ferrous iron transport: the Feo system. FEMS microbiology reviews *40*, 273-298. 10.1093/femsre/fuv049.
Lenth, R.V. (2016). Least-Squares Means: The R Package lsmeans. Journal of Statistical Software *69*, 1 - 33. 10.18637/jss.v069.i01.
Levin, B.R., Moineau, S., Bushman, M., and Barrangou, R. (2013). The population and evolutionary dynamics of phage and bacteria with CRISPR-mediated immunity. PLoS genetics *9*, e1003312. 10.1371/journal.pgen.1003312.
Li, H., Handsaker, B., Wysoker, A., Fennell, T., Ruan, J., Homer, N., Marth, G., Abecasis, G., Durbin, R., and Genome Project Data Processing, S. (2009). The Sequence Alignment/Map format and SAMtools. Bioinformatics *25*, 2078-2079. 10.1093/bioinformatics/btp352.
Li, H., Limenitakis, J.P., Fuhrer, T., Geuking, M.B., Lawson, M.A., Wyss, M., Brugiroux, S., Keller, I., Macpherson, J.A., Rupp, S., et al. (2015). The outer mucus layer hosts a distinct intestinal microbial niche. Nature communications *6*, 8292. 10.1038/ncomms9292.
Liu, D., and Reeves, P.R. (1994). Escherichia coli K12 regains its O antigen. Microbiology (Reading, England) *140 (Pt 1)*, 49-57. 10.1099/13500872-140-1-49.
Lourenço, M., Chaffringeon, L., Lamy-Besnier, Q., Pédron, T., Campagne, P., Eberl, C., Bérard, M., Stecher, B., Debarbieux, L., and De Sordi, L. (2020). The Spatial Heterogeneity of the Gut Limits Predation and Fosters Coexistence of Bacteria and Bacteriophages. Cell host & microbe *28*, 390-401.e395. 10.1016/j.chom.2020.06.002.
Lourenço, M., De Sordi, L., and Debarbieux, L. (2018). The Diversity of Bacterial Lifestyles Hampers Bacteriophage Tenacity. Viruses *10*. 10.3390/v10060327.
Lourenço, M., Ramiro, R.S., Güleresi, D., Barroso-Batista, J., Xavier, K.B., Gordo, I., and Sousa, A. (2016). A Mutational Hotspot and Strong Selection Contribute to the Order of Mutations Selected for during Escherichia coli Adaptation to the Gut. PLoS genetics *12*, e1006420. 10.1371/journal.pgen.1006420.
Love, M.I., Huber, W., and Anders, S. (2014). Moderated estimation of fold change and dispersion for RNA-seq data with DESeq2. Genome biology *15*, 550. 10.1186/s13059-014-0550-8.
Luhachack, L., Rasouly, A., Shamovsky, I., and Nudler, E. (2019). Transcription factor YcjW controls the emergency H(2)S production in E. coli. Nature communications *10*, 2868. 10.1038/s41467-019-10785-x.
Maffei, E., Shaidullina, A., Burkolter, M., Heyer, Y., Estermann, F., Druelle, V., Sauer, P., Willi, L., Michaelis, S., Hilbi, H., et al. (2021). Systematic exploration of Escherichia coli phage-host interactions with the BASEL phage collection. PLoS biology *19*, e3001424. 10.1371/journal.pbio.3001424.
Manrique, P., Dills, M., and Young, M.J. (2017). The Human Gut Phage Community and Its Implications for Health and Disease. Viruses *9*. 10.3390/v9060141.
Martin, M. (2011). Cutadapt removes adapter sequences from high-throughput sequencing reads. 2011 *17*, 3. 10.14806/ej.17.1.200.
Mathieu, A., Dion, M., Deng, L., Tremblay, D., Moncaut, E., Shah, S.A., Stokholm, J., Krogfelt, K.A., Schjørring, S., Bisgaard, H., et al. (2020). Virulent coliphages in 1-year-old children fecal samples are fewer, but more infectious than temperate coliphages. Nature communications *11*, 378. 10.1038/s41467-019-14042-z.
Maura, D., and Debarbieux, L. (2012). On the interactions between virulent bacteriophages and bacteria in the gut. Bacteriophage *2*, 229-233. 10.4161/bact.23557.
Maura, D., Galtier, M., Le Bouguénec, C., and Debarbieux, L. (2012a). Virulent bacteriophages can target O104:H4 enteroaggregative Escherichia coli in the mouse intestine. Antimicrobial agents and chemotherapy *56*, 6235-6242. 10.1128/aac.00602-12.

Maura, D., Morello, E., du Merle, L., Bomme, P., Le Bouguénec, C., and Debarbieux, L. (2012b). Intestinal colonization by enteroaggregative Escherichia coli supports long-term bacteriophage replication in mice. Environmental microbiology *14*, 1844-1854. 10.1111/j.1462-2920.2011.02644.x.

Meadows, J.A., and Wargo, M.J. (2015). Carnitine in bacterial physiology and metabolism. Microbiology (Reading, England) *161*, 1161-1174. 10.1099/mic.0.000080.

Millman, A., Bernheim, A., Stokar-Avihail, A., Fedorenko, T., Voichek, M., Leavitt, A., Oppenheimer-Shaanan, Y., and Sorek, R. (2020). Bacterial Retrons Function In Anti-Phage Defense. Cell *183*, 1551-1561.e1512. 10.1016/j.cell.2020.09.065.

Mirzaei, M.K., and Maurice, C.F. (2017). Ménage à trois in the human gut: interactions between host, bacteria and phages. Nature reviews. Microbiology *15*, 397-408. 10.1038/nrmicro.2017.30.

Mossoro, C., Glaziou, P., Yassibanda, S., Lan, N.T., Bekondi, C., Minssart, P., Bernier, C., Le Bouguénec, C., and Germani, Y. (2002). Chronic diarrhea, hemorrhagic colitis, and hemolytic-uremic syndrome associated with HEp-2 adherent Escherichia coli in adults infected with human immunodeficiency virus in Bangui, Central African Republic. Journal of clinical microbiology *40*, 3086-3088. 10.1128/jcm.40.8.3086-3088.2002.

Nachin, L., Nannmark, U., and Nyström, T. (2005). Differential roles of the universal stress proteins of Escherichia coli in oxidative stress resistance, adhesion, and motility. Journal of bacteriology *187*, 6265-6272. 10.1128/jb.187.18.6265-6272.2005.

Otto, K., Norbeck, J., Larsson, T., Karlsson, K.A., and Hermansson, M. (2001). Adhesion of type 1-fimbriated Escherichia coli to abiotic surfaces leads to altered composition of outer membrane proteins. Journal of bacteriology *183*, 2445-2453. 10.1128/jb.183.8.2445-2453.2001.

Pires, D.P., Melo, L.D.R., and Azeredo, J. (2021). Understanding the Complex Phage-Host Interactions in Biofilm Communities. Annu Rev Virol *8*, 73-94. 10.1146/annurev-virology-091919-074222.

Radke, K.L., and Siegel, E.C. (1971). Mutation preventing capsular polysaccharide synthesis in Escherichia coli K-12 and its effect on bacteriophage resistance. Journal of bacteriology *106*, 432-437. 10.1128/jb.106.2.432-437.1971.

Rousset, F., Dowding, J., Bernheim, A., Rocha, E.P.C., and Bikard, D. (2021). Prophage-encoded hotspots of bacterial immune systems. bioRxiv, 2021.2001.2021.427644. 10.1101/2021.01.21.427644.

Sausset, R., Petit, M.A., Gaboriau-Routhiau, V., and De Paepe, M. (2020). New insights into intestinal phages. Mucosal immunology *13*, 205-215. 10.1038/s41385-019-0250-5.

Scanlan, J.G., Hall, A.R., and Scanlan, P.D. (2019). Impact of bile salts on coevolutionary dynamics between the gut bacterium Escherichia coli and its lytic phage PP01. Infection, genetics and evolution : journal of molecular epidemiology and evolutionary genetics in infectious diseases *73*, 425-432. 10.1016/j.meegid.2019.05.021.

Shin, H., Lee, J.H., Kim, H., Choi, Y., Heu, S., and Ryu, S. (2012). Receptor diversity and host interaction of bacteriophages infecting Salmonella enterica serovar Typhimurium. PloS one *7*, e43392. 10.1371/journal.pone.0043392.

Shkoporov, A.N., Clooney, A.G., Sutton, T.D.S., Ryan, F.J., Daly, K.M., Nolan, J.A., McDonnell, S.A., Khokhlova, E.V., Draper, L.A., Forde, A., et al. (2019). The Human Gut Virome Is Highly Diverse, Stable, and Individual Specific. Cell host & microbe *26*, 527-541.e525. 10.1016/j.chom.2019.09.009.

Sillankorva, S., Oliveira, R., Vieira, M.J., Sutherland, I., and Azeredo, J. (2004). Pseudomonas fluorescens infection by bacteriophage PhiS1: the influence of temperature, host growth phase and media. FEMS microbiology letters *241*, 13-20. 10.1016/j.femsle.2004.06.058.

Szklarczyk, D., Gable, A.L., Lyon, D., Junge, A., Wyder, S., Huerta-Cepas, J., Simonovic, M., Doncheva, N.T., Morris, J.H., Bork, P., et al. (2019). STRING v11: protein-protein association networks with increased coverage, supporting functional discovery in genome-wide experimental datasets. Nucleic acids research *47*, D607-d613. 10.1093/nar/gky1131.

Toliver-Kinsky, T., Cui, W., Törö, G., Lee, S.J., Shatalin, K., Nudler, E., and Szabo, C. (2019). H(2)S, a Bacterial Defense Mechanism against the Host Immune Response. Infection and immunity *87*. 10.1128/iai.00272-18.

Touchon, M., Hoede, C., Tenaillon, O., Barbe, V., Baeriswyl, S., Bidet, P., Bingen, E., Bonacorsi, S., Bouchier, C., Bouvet, O., et al. (2009). Organised genome dynamics in the Escherichia coli species results in highly diverse adaptive paths. PLoS genetics *5*, e1000344. 10.1371/journal.pgen.1000344.

Varet, H., Brillet-Guéguen, L., Coppée, J.Y., and Dillies, M.A. (2016). SARTools: A DESeq2- and EdgeR-Based R Pipeline for Comprehensive Differential Analysis of RNA-Seq Data. PloS one *11*, e0157022. 10.1371/journal.pone.0157022.

Vidakovic, L., Singh, P.K., Hartmann, R., Nadell, C.D., and Drescher, K. (2018). Dynamic biofilm architecture confers individual and collective mechanisms of viral protection. Nature microbiology *3*, 26-31. 10.1038/s41564-017-0050-1.

Weintraub, A. (2007). Enteroaggregative Escherichia coli: epidemiology, virulence and detection. Journal of medical microbiology *56*, 4-8. 10.1099/jmm.0.46930-0.

Weiss, M., Denou, E., Bruttin, A., Serra-Moreno, R., Dillmann, M.L., and Brüssow, H. (2009). In vivo replication of T4 and T7 bacteriophages in germ-free mice colonized with Escherichia coli. Virology *393*, 16-23. 10.1016/j.virol.2009.07.020.

Woods, S.A., and Guest, J.R. (1987). Differential roles of the Escherichia coli fumarases and fnr-dependent expression of fumarase B and aspartase. FEMS microbiology letters *48*, 219-224. 10.1111/j.1574-6968.1987.tb02545.x.

Xavier, K.B., and Bassler, B.L. (2005). Regulation of uptake and processing of the quorum-sensing autoinducer AI-2 in Escherichia coli. Journal of bacteriology *187*, 238-248. 10.1128/jb.187.1.238-248.2005.

Zuo, T., Sun, Y., Wan, Y., Yeoh, Y.K., Zhang, F., Cheung, C.P., Chen, N., Luo, J., Wang, W., Sung, J.J.Y., et al. (2020). Human-Gut-DNA Virome Variations across Geography, Ethnicity, and Urbanization. Cell host & microbe *28*, 741-751.e744. 10.1016/j.chom.2020.08.005.

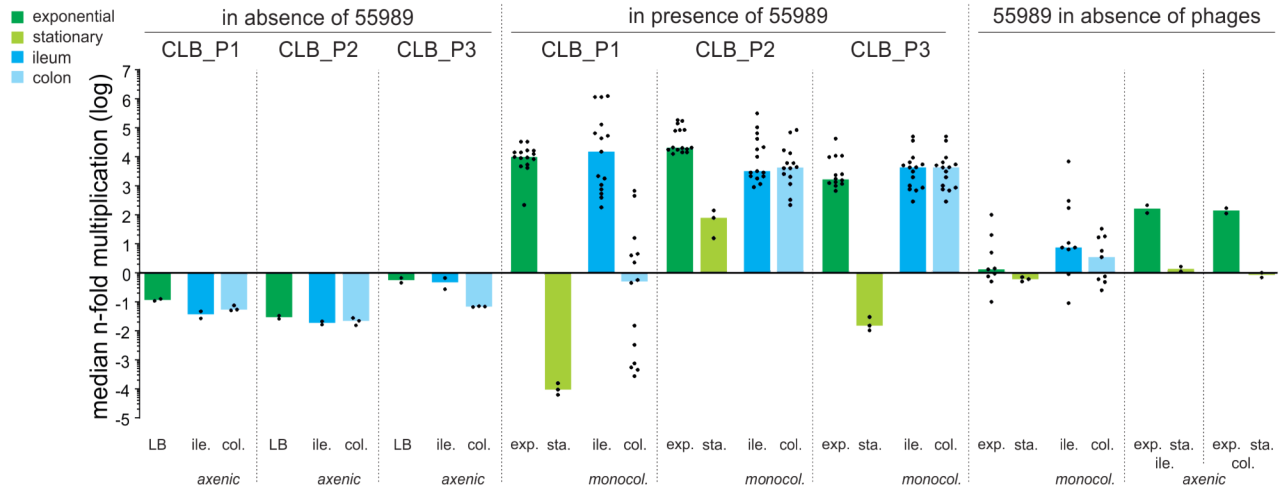
exponential
stationary
ileum
colon
in absence of 55989
in presence of 55989
55989 in absence of phages
CLB_P1
CLB_P2
CLB_P3
median n-fold multiplication (log)
7
6
5
4
3
2
1
0
-1
-2
-3
-4
-5
LB
ile.
col.
exp.
sta.
axenic
monocol.

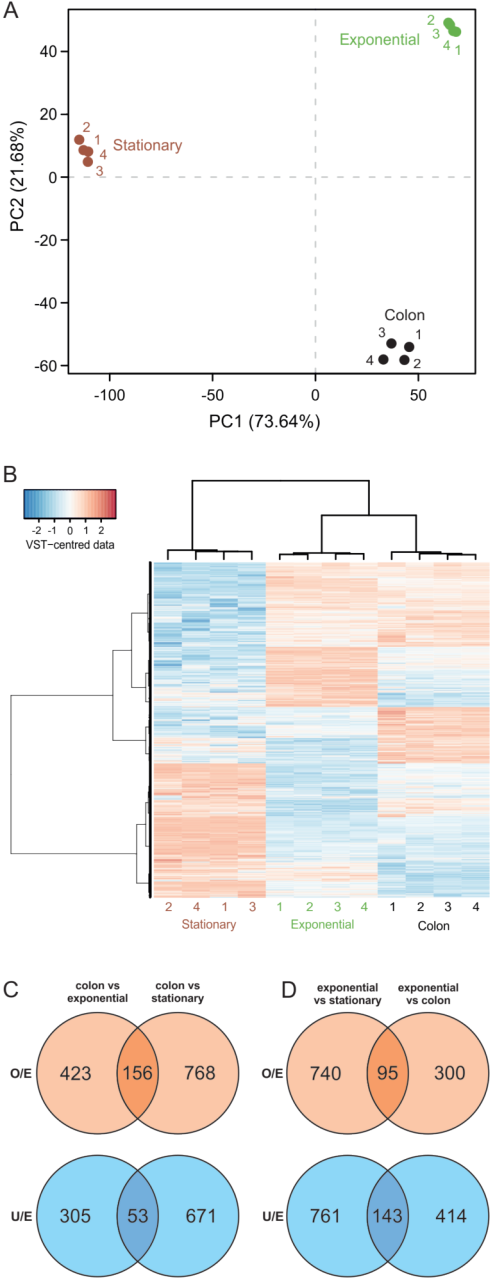
A
Exponential
2
3
4
1
Stationary
2
1
4
3
Colon
3
1
4
2
PC2 (21.68%)
PC1 (73.64%)
40
20
0
-20
-40
-60
-100
-50
0
50
B
-2 -1 0 1 2
VST−centred data
2 4 1 3
Stationary
1 2 3 4
Exponential
1 2 3 4
Colon
C
colon vs exponential
colon vs stationary
O/E
423
156
768
U/E
305
53
671
D
exponential vs stationary
exponential vs colon
O/E
740
95
300
U/E
761
143
414

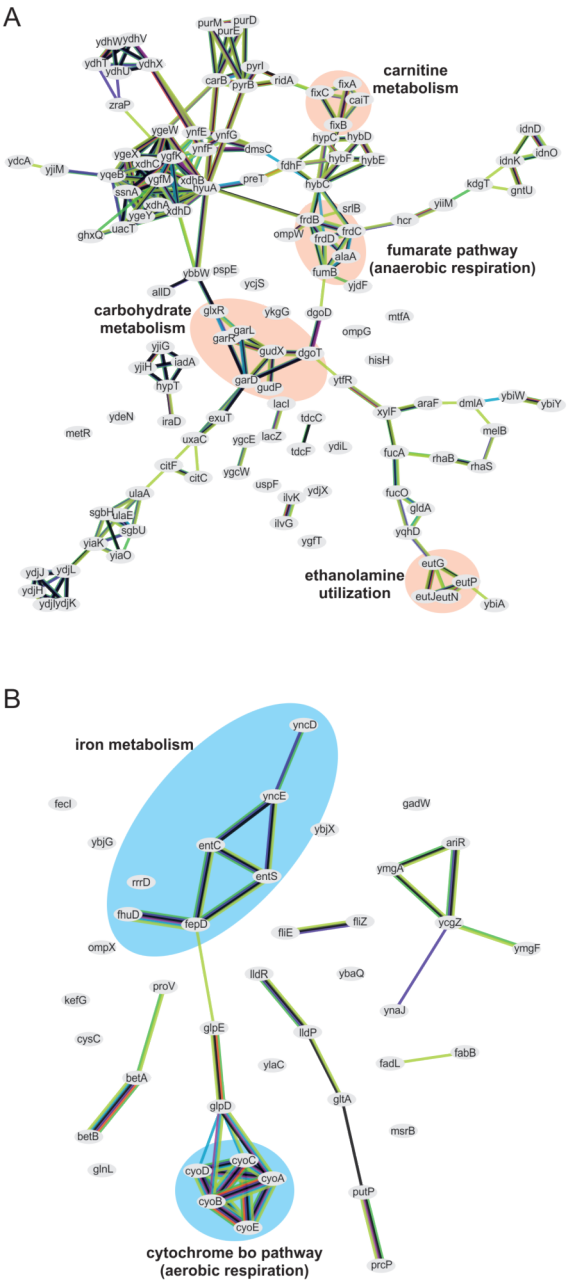
A
carnitine metabolism
fumarate pathway (anaerobic respiration)
carbohydrate metabolism
ethanolamine utilization
purM
purD
purE
ydhW
ydhV
ydhT
ydhU
ydhX
zraP
carB
pyrB
pyrI
ridA
fixA
fixC
caiT
fixB
hypC
hybD
hybF
hybE
hybC
fdhF
dmsC
ygeW
ynfE
ynfG
ygeX
ygfK
ynfF
ydcA
yjiM
yqeB
xdhC
xdhB
hyuA
preT
ssnA
ygfM
xdhA
ygeY
xdhD
ghxQ
uacT
idnD
idnO
idnK
kdgT
gntU
yiiM
hcr
srlB
frdB
frdC
ompW
frdD
alaA
fumB
ydjF
pspE
ycjS
ybbW
allD
glxR
garL
garR
ykgG
dgoD
mtfA
ompG
gudX
dgoT
hisH
yjiG
yjiH
iadA
hypT
garD
gudP
ytfR
ydeN
iraD
exuT
lacI
tdcC
araF
dmlA
ybiW
ybiY
metR
uxaC
ygcE
lacZ
tdcF
ydiL
xylF
melB
fucA
rhaB
rhaS
citF
citC
ygcW
uspF
ydjX
ilvK
ilvG
ygfT
fucO
gldA
yqhD
ulaA
sgbH
ulaE
sgbU
ylaK
yiaO
ydjJ
ydjL
ydjH
ydjIydjK
eutG
eutP
eutJeutN
ybiA
B
iron metabolism
yncD
yncE
fecI
ybjX
ybjG
entC
entS
rrrD
fhuD
fepD
ompX
gadW
ariR
ymgA
ycgZ
ymgF
fliE
fliZ
lldR
ybaQ
ynaJ
kefG
proV
glpE
lldP
cysC
ylaC
fadL
fabB
betA
gltA
glpD
msrB
betB
glnL
cyoD
cyoC
cyoA
cyoB
cyoE
putP
prcP
cytochrome bo pathway (aerobic respiration)

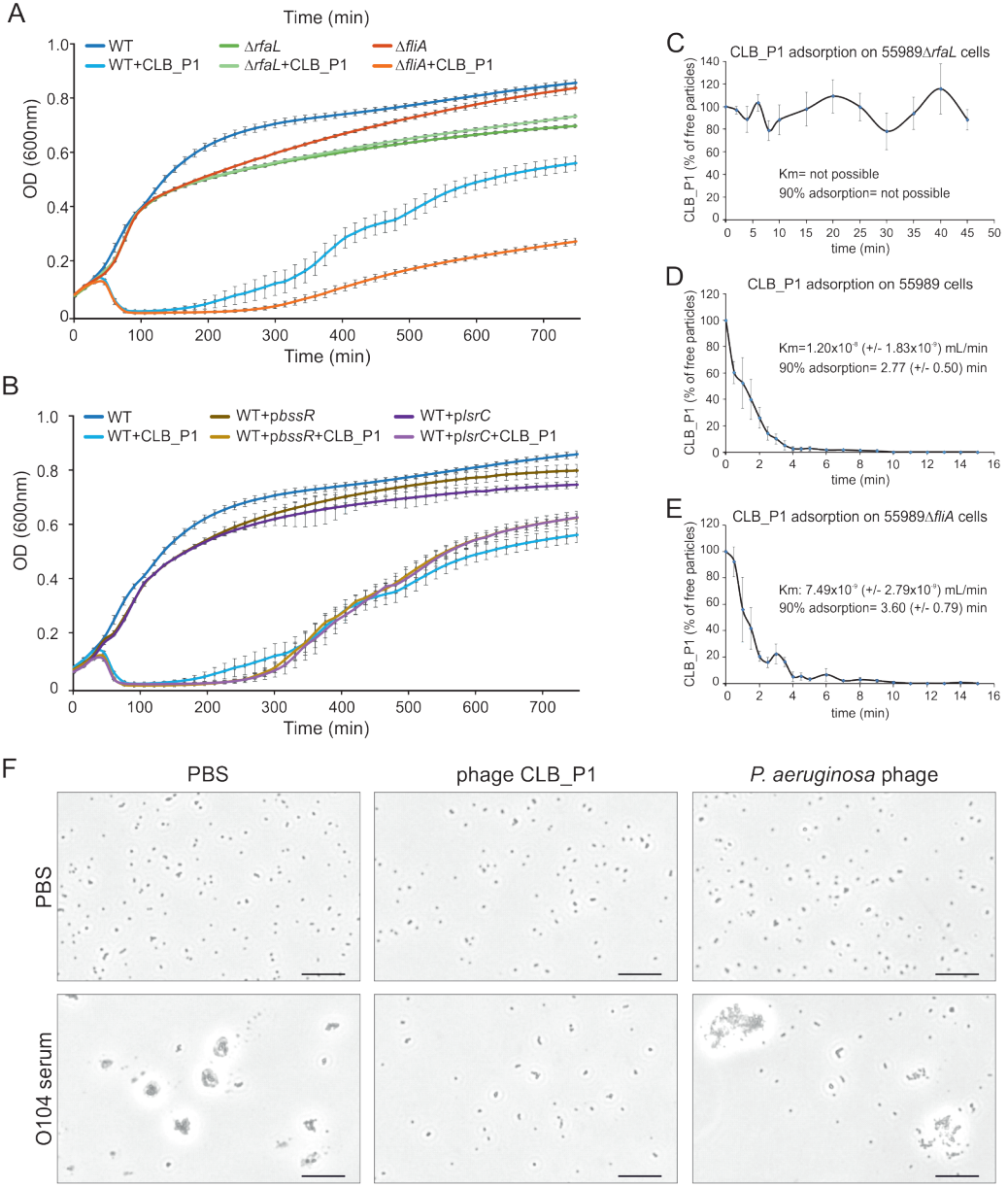
A
Time (min)
WT
WT+CLB_P1
ΔrfaL
ΔrfaL+CLB_P1
ΔfliA
ΔfliA+CLB_P1
OD (600nm)
Time (min)
B
WT
WT+CLB_P1
WT+pbssR
WT+pbssR+CLB_P1
WT+plsrC
WT+plsrC+CLB_P1
OD (600nm)
Time (min)
C
CLB_P1 adsorption on 55989ΔrfaL cells
CLB_P1 (% of free particles)
Km= not possible
90% adsorption= not possible
time (min)
D
CLB_P1 adsorption on 55989 cells
CLB_P1 (% of free particles)
Km=1.20x10-8 (+/- 1.83x10-8) mL/min
90% adsorption= 2.77 (+/- 0.50) min
time (min)
E
CLB_P1 adsorption on 55989ΔfliA cells
CLB_P1 (% of free particles)
Km: 7.49x10-9 (+/- 2.79x10-9) mL/min
90% adsorption= 3.60 (+/- 0.79) min
time (min)
F
PBS
phage CLB_P1
P. aeruginosa phage
PBS
O104 serum

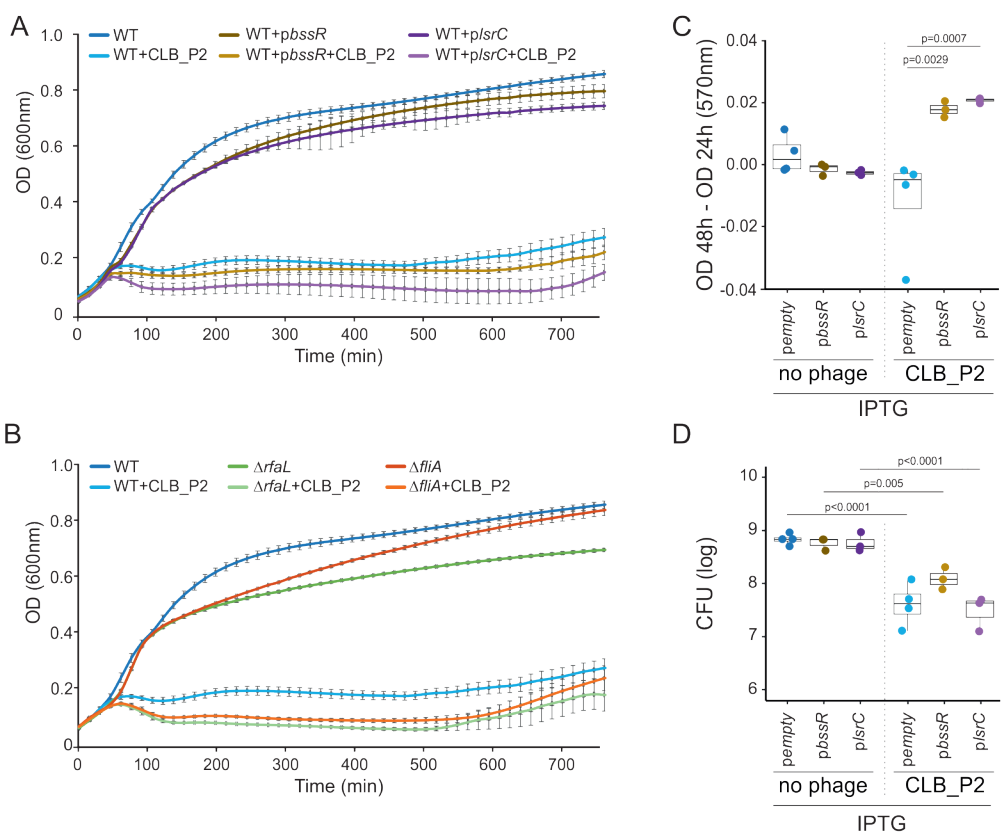
A
WT
WT+CLB_P2
WT+pbssR
WT+pbssR+CLB_P2
WT+plsrC
WT+plsrC+CLB_P2
OD (600nm)
Time (min)
B
WT
WT+CLB_P2
ΔrfaL
ΔrfaL+CLB_P2
ΔfliA
ΔfliA+CLB_P2
OD (600nm)
Time (min)
C
OD 48h - OD 24h (570nm)
p=0.0007
p=0.0029
pempty
pbssR
plsrC
no phage
CLB_P2
IPTG
D
CFU (log)
p<0.0001
p=0.005
p<0.0001
pempty
pbssR
plsrC
no phage
CLB_P2
IPTG

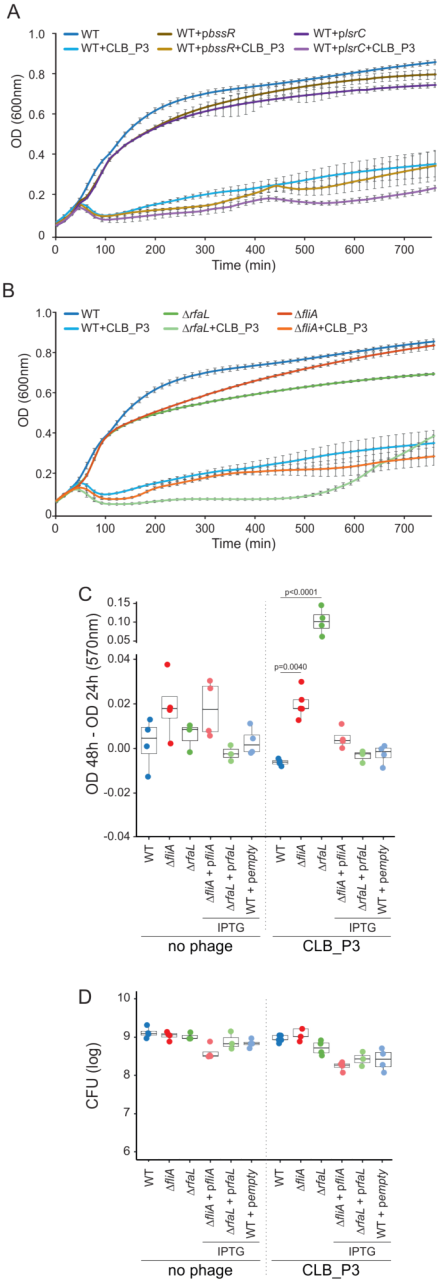
A
WT
WT+CLB_P3
WT+pbssR
WT+pbssR+CLB_P3
WT+plsrC
WT+plsrC+CLB_P3
OD (600nm)
Time (min)
B
WT
WT+CLB_P3
ΔrfaL
ΔrfaL+CLB_P3
ΔfliA
ΔfliA+CLB_P3
OD (600nm)
Time (min)
C
OD 48h - OD 24h (570nm)
p<0.0001
p=0.0040
WT
ΔfliA
ΔrfaL
ΔfliA + pfliA
ΔrfaL + prfaL
WT + pempty
IPTG
no phage
CLB_P3
D
CFU (log)
WT
ΔfliA
ΔrfaL
ΔfliA + pfliA
ΔrfaL + prfaL
WT + pempty
IPTG
no phage
CLB_P3

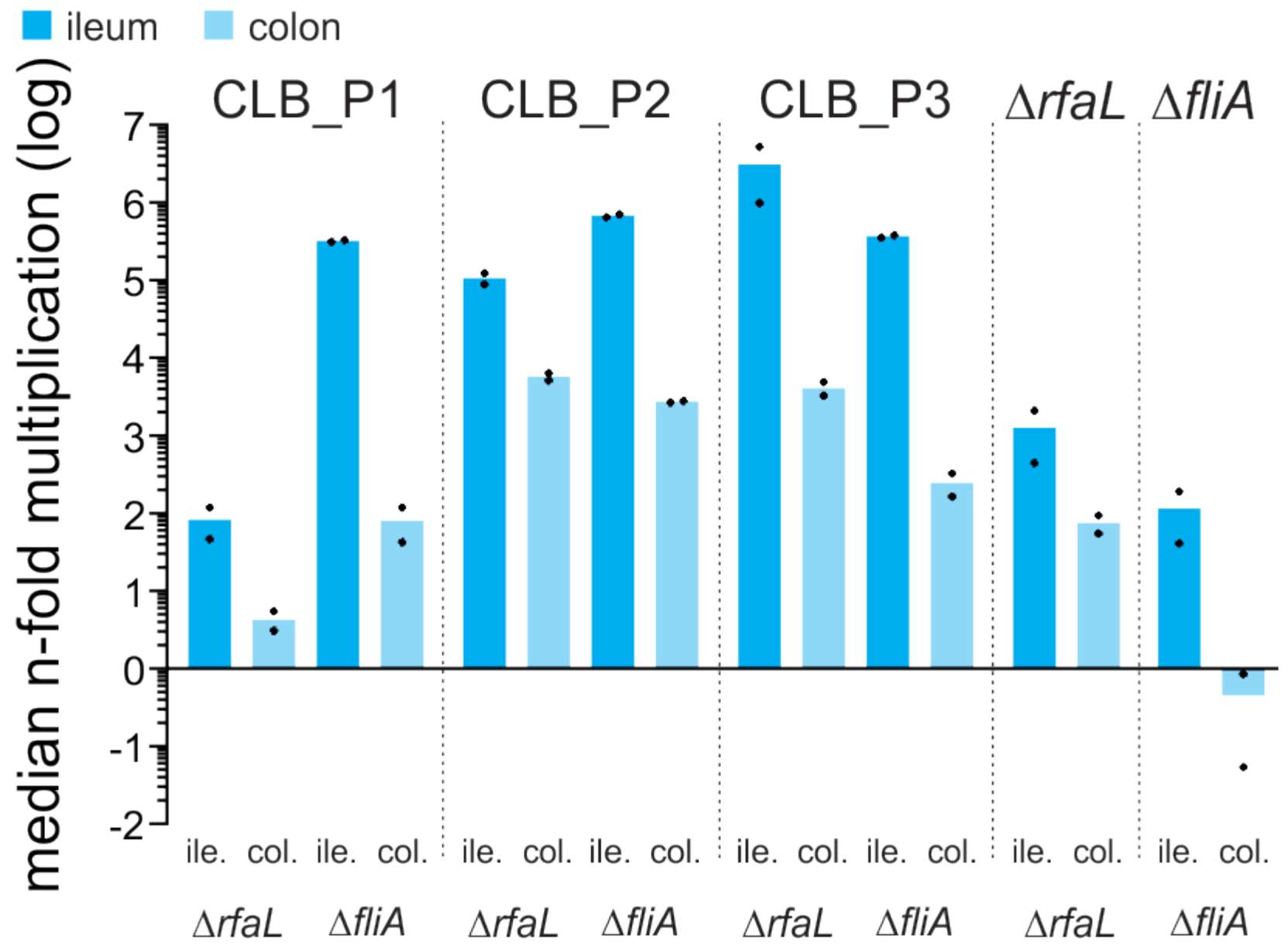
ileum
colon
CLB_P1
CLB_P2
CLB_P3
ΔrfaL
ΔfliA
median n-fold multiplication (log)
7
6
5
4
3
2
1
0
-1
-2
ile.
col.
ΔrfaL
ΔfliA

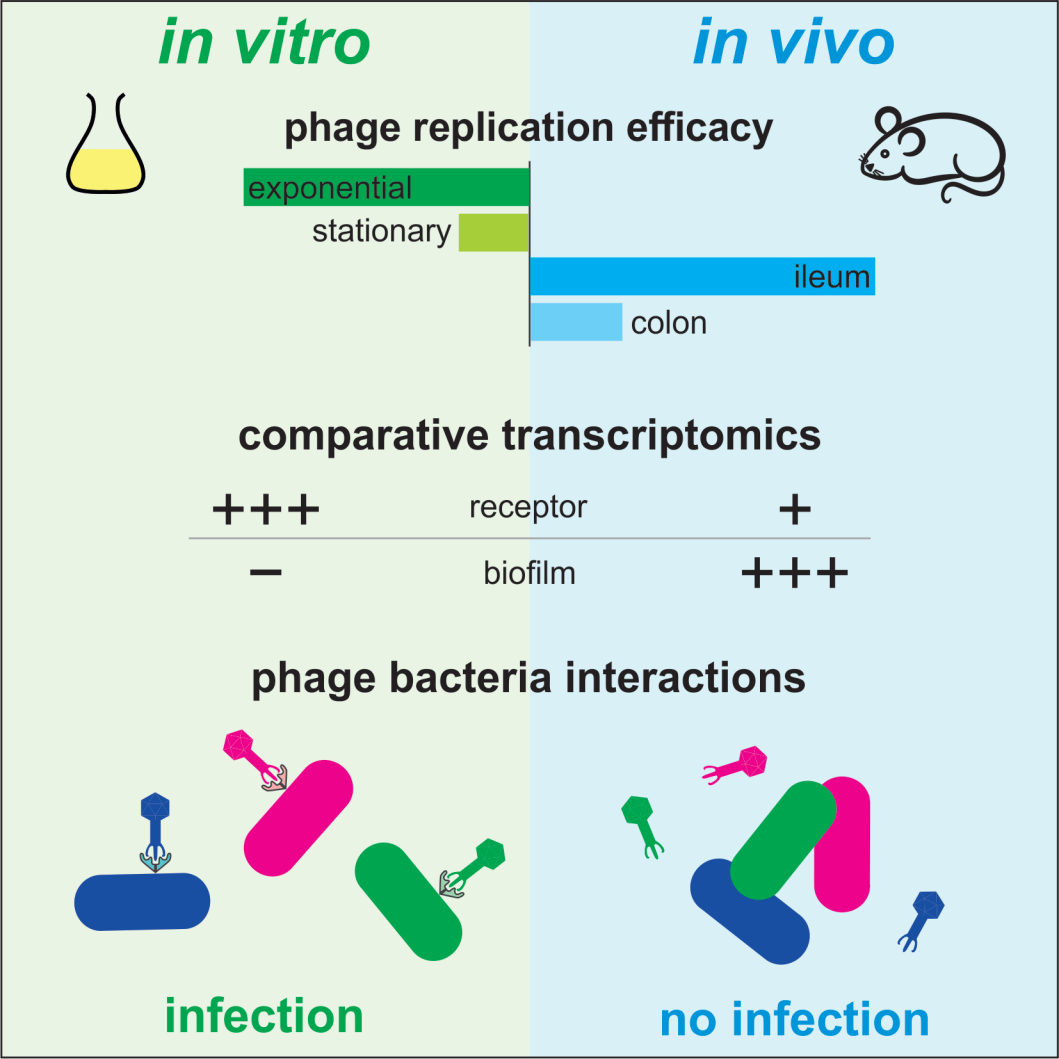
in vitro
in vivo
phage replication efficacy
exponential
stationary
ileum
colon
comparative transcriptomics
+++
receptor
+
−
biofilm
+++
phage bacteria interactions
infection
no infection